

NASA-CR-169,882

NASA-CR-169882
19830012873

FIFTH SEMI-ANNUAL PROGRESS REPORT

Evaluation of High Temperature Structural Adhesives for Extended Service

CONTRACT NAS1-15605

SUBMITTED TO
NATIONAL AERONAUTICS AND SPACE ADMINISTRATION
LANGLEY RESEARCH CENTER

LIBRARY COPY

OCT 28 1981

LANGLEY RESEARCH CENTER
LIBRARY, NASA
HAMPTON, VIRGINIA

MAY 1981



NF02605

THE BOEING AEROSPACE COMPANY
POST OFFICE BOX 3999
SEATTLE, WASHINGTON 98124

SIXTH SEMI-ANNUAL PROGRESS REPORT

Evaluation of High Temperature Structural Adhesives for Extended Service

CONTRACT NAS1-15605

SUBMITTED TO
NATIONAL AERONAUTICS AND SPACE ADMINISTRATION
LANGLEY RESEARCH CENTER

NOVEMBER 1981

THE BOEING AEROSPACE COMPANY
POST OFFICE BOX 3999
SEATTLE, WASHINGTON 98124

1183-21142 #

TABLE OF CONTENTS

	<u>Page</u>
1.0 INTRODUCTION	3
2.0 TECHNICAL DISCUSSION	8
2.1 PHASE I--SURFACE TREATMENT STUDY	8
2.2 PHASE I--SURFACE CHARACTERIZATION AND FAILURE ANALYSIS	8
2.2.1 Introduction	8
2.2.2 Analytical Techniques	9
2.2.2.1 Scanning Electron Microscopy	9
2.2.2.2 Surface Chemical Analysis	9
2.2.3 Technical Discussion	10
2.2.3.1 Baseline Studies	10
2.2.3.2 Analysis of Failed Specimens	16
2.2.4 Summary	57
2.2.4.1 Results	57
2.2.5 Discussion	59
2.2.5.1 General Behavior	61
2.2.5.2 General Discussion of Results	61
2.2.5.3 Conclusions	63
2.3 PHASE II--TASK II ENVIRONMENTAL EXPOSURE DATA	63
2.3.1 General Discussion	63
2.3.2 Stressed Thermal Aging	65
2.3.3 Humidity Exposure	65
2.3.4 Aircraft Fluid Exposure	65
2.3.5 Extended Exposure	68
2.3.6 Thermal Cycling	68
3.0 PROGRAM STATUS	71
3.1 PHASE I--ADHESIVE SCREENING	71
3.2 PHASE II--ADHESIVE OPTIMIZATION AND CHARACTERIZATION	72

TABLE OF CONTENTS (Continued)

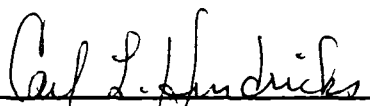
	<u>Page</u>
4.0 WORK PLANNED FOR NEXT 6 MONTHS	73
REFERENCES	74


FOREWORD

This report was prepared by the Boeing Aerospace Company, Kent, Washington, under Contract NAS1-15605, "Evaluation of High Temperature Structural Adhesives for Extended Service." It is the sixth semi-annual technical progress report detailing work performed between 2 May 1981 and 2 November 1981. The program is sponsored by the National Aeronautics and Space Administration, Langley Research Center (NASA-LRC). Mr. J. B. Nelson is the project monitor for NASA-LRC.

Performance of this contract is under the direction of the Materials Technology department of the Boeing Aerospace Company. Mr. J. C. Johnson is program manager and Mr. C. L. Hendricks is technical leader. Mr. S. G. Hill is principal investigator. Major contributors to this program are:

Patricia Peters	Surface Morphology and Characterization
Brian Smith	Surface Characterization
Brian McElroy	Surface Characterization
Gene Ledbury	Surface Characterization
William Dumars	Materials and Processes
Julie Vry	Materials and Processes
Ralph Hodges	Materials and Processes
Gene Carlson	Materials and Processes

Prepared by 
C. L. Hendricks
Technical Leader

Approved by 
J. C. Johnson
Program Support

SUMMARY

This report describes the Phase I Surface Characterization and Failure Analysis of lap shear bond failures occurring with the adhesive systems consisting of:

- o LARC-13 Adhesive, Pasa Jell Surface Treatment on Titanium
- o LARC-13 Adhesive, 10 Volt CAA Treatment on Titanium
- o PPQ Adhesive, 10 Volt CAA Treatment on Titanium
- o PPQ Adhesive, 5 Volt CAA Treatment on Titanium

The failure analysis concentrated on the 10,000 hr. 505K (450°F) exposed specimens which exhibited classic adhesive failure. Cause of bond failure was attributed to resin/oxide interface pull-out and separation during shear test.

Phase II efforts described in this report cover environmental exposure data being generated on the PPQ - 10 Volt CAA and LARC-TPI-10 Volt CAA adhesive systems.

1.0 INTRODUCTION

Contract NAS1-15605 is a NASA-LRC program to develop technology to support Supersonic Cruise Research (SCR). The primary objective of this contract is to evaluate and select adhesive systems for SCR applications and demonstrate elevated-temperature environmental durability for extended periods (approximately 50,000 hours). Boeing's development approach is to evaluate leading adhesive resins and surface preparation techniques for bonding titanium structure, optimize processes, and establish durable adhesive systems (adhesive, surface preparation, and primer) capable of extended service at 505K (450°F).

Program efforts are divided into two phases. Phase I, Adhesive Screening, is a 12-month study to evaluate ten adhesive resins and eight titanium surface treatments, resulting in the selection of two adhesive systems for more extensive evaluation. Phase II, Adhesive Optimization and Characterization, is an optional 24-month study dependent upon successful results from Phase I. It is divided into two tasks. Task I optimizes the two selected systems, provides necessary specifications, and generates a moderate data base. Figures 1-1 and 1-2 illustrate the program flow for Phases I and II, respectively. Figures 1-3 and 1-4 show Phase I and II significant events and schedules, respectively.

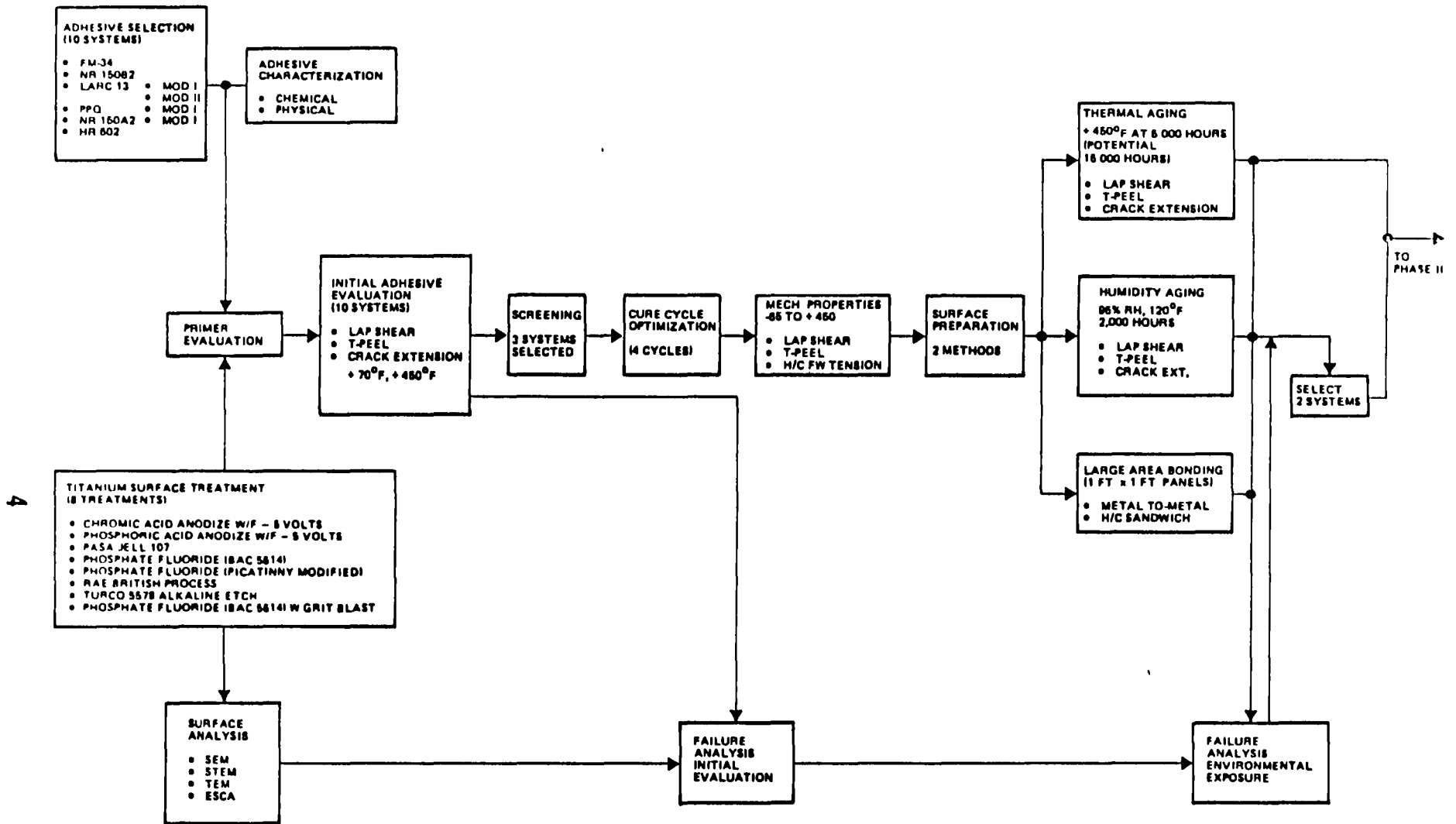


Figure 1-1: Phase I, Flow Diagram

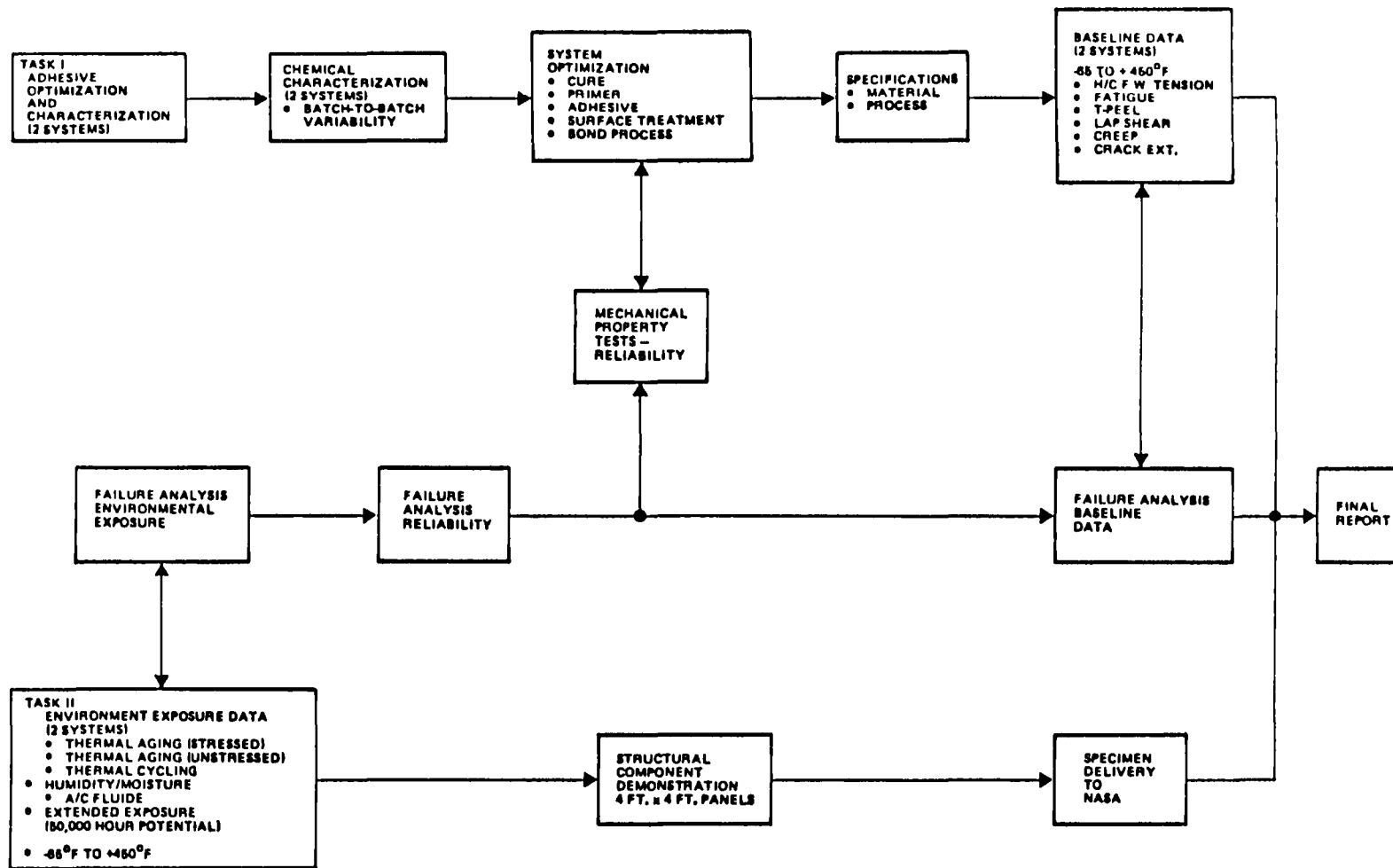


Figure 1-2: Phase II, Adhesive Optimization and Characterization Flow Diagram

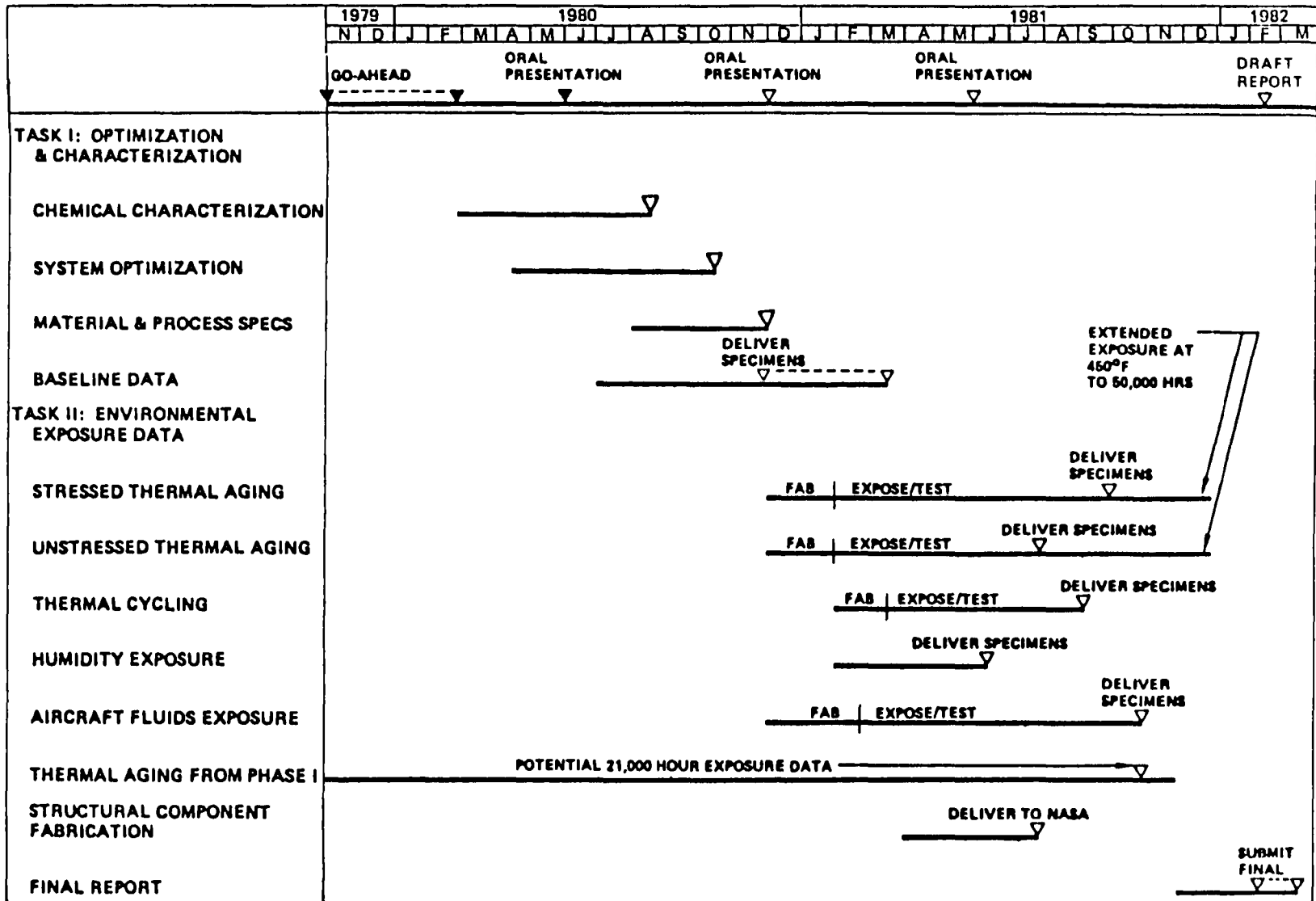


Figure 1-4: Program Schedule Phase II, Adhesive Optimization and Characterization

2.0 TECHNICAL DISCUSSION

2.1 PHASE I—SURFACE TREATMENT STUDY

This portion of the program is evaluating the effects of 322K (120°F)/95% relative humidity (RH) and 505K (450°F) thermal aging on two different titanium surface treatments for each of the three adhesives.

LARC-13 surface treatments are:

- o Pasa-Jell 107
- o Chromic acid anodize, 10 volts

NR056X surface treatments are:

- o Pasa-Jell 107
- o Chromic acid anodize, 10 volts

PPQ surface treatments are:

- o Chromic acid anodize, 5 volts
- o Chromic acid anodize, 10 volts

Test coupons for PPQ are currently between 10,000 and 20,000 hours aging at 505K (450°F). Data for 10,000 hours was presented in the May 1981 semi-annual report.

2.2 PHASE I—SURFACE CHARACTERIZATION AND FAILURE ANALYSIS

2.2.1 Introduction

The May 1981 semi-annual report described an abrupt change in PPQ and LARC-13 bonded coupons from cohesive failure after 5,000 hours at 505K (450°F) to adhesive failure at 10,000 hours at 505K (450°F). To explain the change in failure mode an in-depth surface characterization and failure analysis was conducted as part of the overall program efforts. This section describes the analytical techniques and results of this study.

2.2.2 Analytical Techniques

Electron microscopical and surface chemical analysis techniques were employed to characterize surface failure areas of bonded titanium coupons. Each technique will be described briefly, together with the instruments used.

2.2.2.1 Scanning Electron Microscopy (SEM/STEM)

For surface morphology studies of titanium oxides and failed lap-shear specimens, an SEM technique was used. Improved resolution can be obtained by using a secondary electron imaging technique in a scanning transmission electron microscope (STEM). A detailed discussion of the comparison between the capabilities of the two instruments was reported in the Third Semi-Annual Progress Report (May 1980). The disadvantages of the STEM reported there are due to the difficulty of specimen preparation, particularly limitations on specimen size. The superior resolution of the STEM, however, made it essential for use in this study.

Specimens were prepared for analysis either in a plan-view mode or as a profile view of a fractured oxide. Boeing has developed techniques for applying conductive coatings to specimens that have resulted in significant improvements in resolution (ref. 1). Roughly 5 nm of Au/Pd is vapor-deposited onto the surface of the specimen.

A JEOL JEM 100C belonging to the University of Washington was used by Boeing personnel. Also available on the instrument is an energy-dispersive X-ray elemental analysis (EDX) capability. EDX was used with the STEM in the transmission electron microscope (TEM) mode, for analysis of thin sections. Thin sections (~ 50 nm thick) were cut on a Sorval MT2B ultramicrotome using a 55 $^{\circ}$ diamond knife. EDX analysis of a thin section gives a detection limit of 1:10,000 for elements of atomic number > 11 .

2.2.2.2 Surface Chemical Analysis (AES; ESCA)

For surface chemical analysis studies, two techniques were used: Auger electron spectroscopy (AES) and electron spectroscopy for chemical analysis (ESCA). Both techniques were performed in the same instrument, a Physical Electronics ESCA-SAM spectrometer, Model 550. The techniques were described in the Third Semi-Annual

Progress Report (May 1980).

The elemental surface composition of the failed lap-shear surfaces may be determined by ESCA. Using this technique, the failure locus of the lap shear can be inferred through elemental fingerprinting to within a 10 nm depth over a wide area (4mm²).

To map the distribution of elements with a lateral resolution of 5 μ m AES is used. The technique is useful for analysis with a maximum depth of penetration of 10 nm.

ESCA can be used for elemental analysis, can be used on polymers, and also gives an indication of chemical state. AES, with better spatial resolution, can also be used for elemental analysis. The usefulness of AES for polymer analysis is limited by problems of charging with the minimum current densities required.

2.2.3 Technical Discussion

2.2.3.1 Baseline Studies

Objectives

A limited amount of baseline study was undertaken during the current phase. The purpose of baseline studies generally is to characterize the materials systems undisturbed by other processes, such as bonding, aging, and mechanical testing, for further comparisons after processing. Specifically, one set of baseline samples was characterized because of earlier irregularities in microstructure of the oxide; the present study characterized a 10V CAA oxide produced from a fresh anodizing solution, and the primer infiltration into this more representative oxide structure.

Morphological studies were performed with the University of Washington STEM. Samples were examined in both the plan view and transversely fractured profile view. The intent was to delineate the oxide cell structure and surface area available for mechanical bonding of the primer/adhesive systems in use. Some pitfalls in conducting so-called baseline studies are the following:

- o Artifacts produced from Au-Pd conductive coating for SEM/STEM analyses are not well understood, but probably limit ultrastructural resolution and influence apparent pore and cell sizes.

- o The inherently laborious nature of these studies precludes exhaustive characterizations such as the influences of anodizing voltages, bath conditions, or thermal aging of bare oxides.

Observations of the bare oxide and primer penetration into baseline oxide samples are summarized.

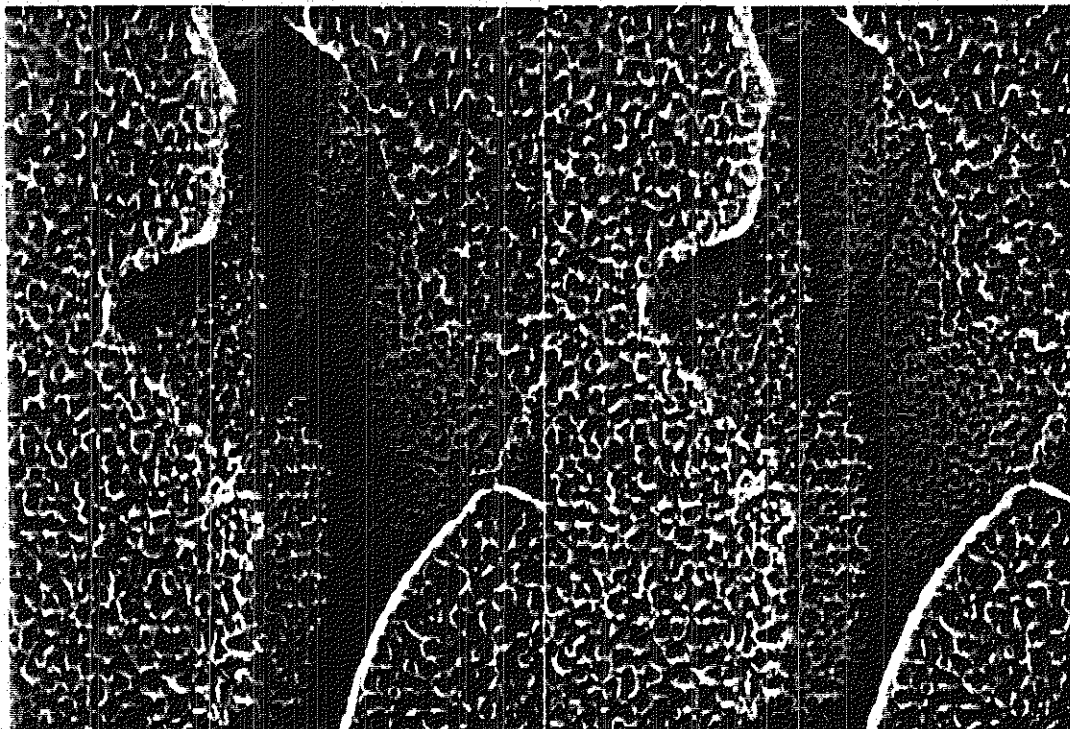
Oxide Morphology, 10V CAA

The plan view of a 10V CAA oxide (Figure 2.2.3.1-1) shows the top of the oxide with the oxide pores, approximately 30 nm in diameter, clearly in view. The lab-fractured view of the oxide (Figure 2.2.3.1-2) shows that the oxide has a columnar structure with a depth of about 120 nm. This fractured view of a recently prepared specimen is consistent with Figure 2.4.3-26 of the third semi-annual report. A significant difference between the two oxides, however, is the formation of a contaminant or duplex oxide just above the base oxide in Figure 2.4.3-26 (prior report). The base oxide is that oxide adjacent to the base metal. The base oxides in the above two figures (Figure 2.4.3-26 and Figure 3.1-2) have the same appearance and approximately the same thickness. The duplex structure shown in the third semi-annual report was a result of the solutions in the preparation bath being degraded. When this structure was noticed, new specimens were prepared with fresh chemicals, and a single-layer base oxide resulted. The specimens prepared from the fresh chemicals resulted in increased mechanical strengths during lap-shear analysis.

Baseline Primer Penetration Study, 10V CAA

To determine the degree of primer penetration into the oxide layer, a control specimen was prepared in which primer was applied to the oxide surface, without exposure to environmental effects. PPQ was selected as the primer for the control penetration study. Interpretation of lap-shear failure analysis data required baseline knowledge of the degree of primer penetration into a fresh oxide specimen.

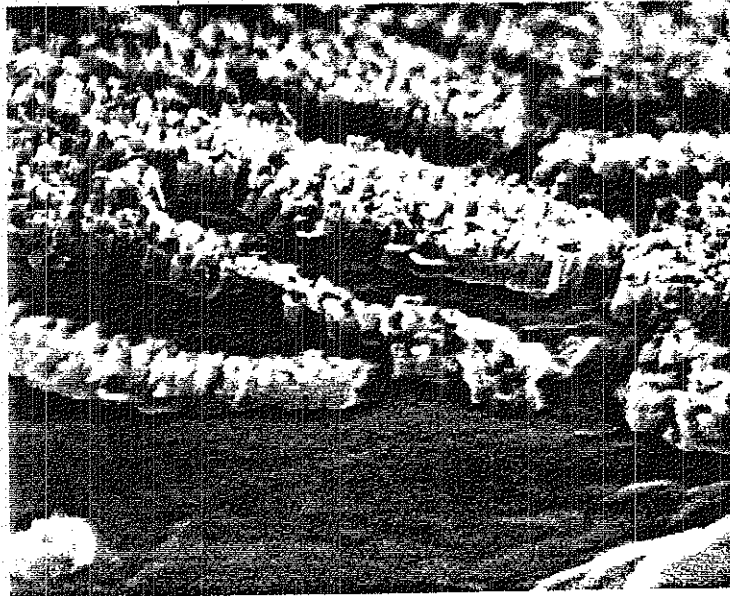
Figure 2.2.3.1-3 is a stereographic pair of a fractured specimen, showing the primer penetrating to the base of the oxide. Figure 2.2.3.1-4 is a stereographic pair of another region of the fractured specimen. These micrographs show the primer being incompletely pulled away from the top of the oxide layer. This pulling away of the



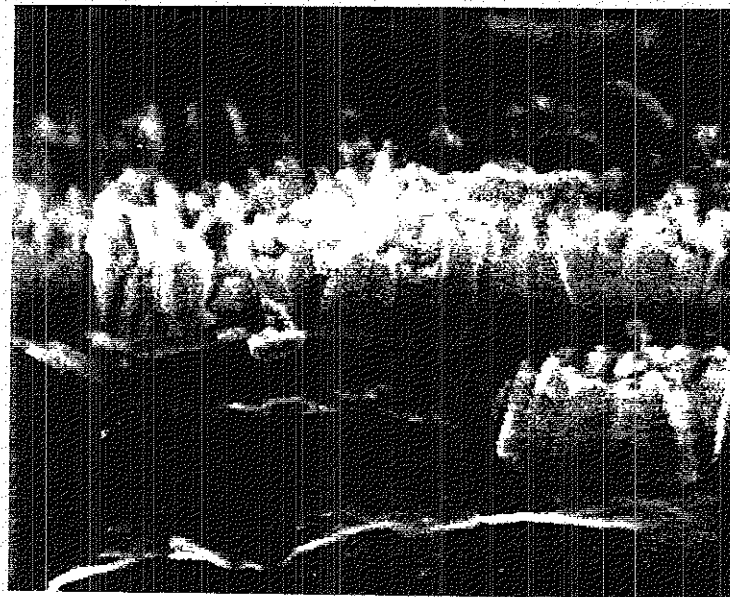
0.5 micrometer

10 V CAA AS ANODIZED - NO ADDITIONAL PROCESSING
STEREO PAIR TOP VIEW SHOWING
OXIDE PORES (~ 30NM IN DIAMETER).

Figure 2.2.3.1-1



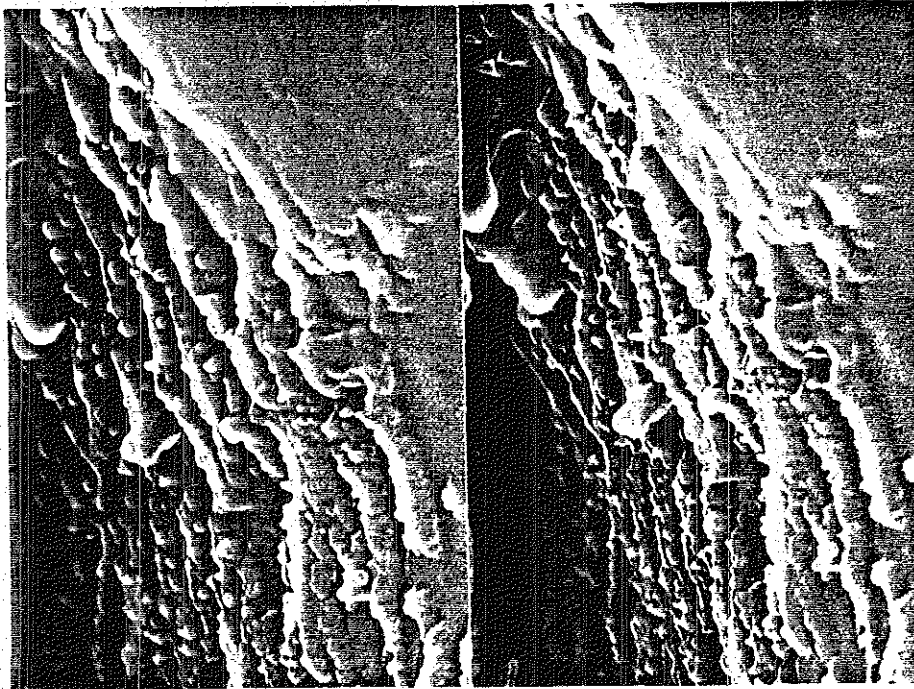
0.5 micrometer



0.2 micrometer

10V CAA AS ANODIZED - NO ADDITIONAL PROCESSING
THE OXIDE HAS A COLUMNAR STRUCTURE
WITH A THICKNESS OF $\sim 120\text{NM}$

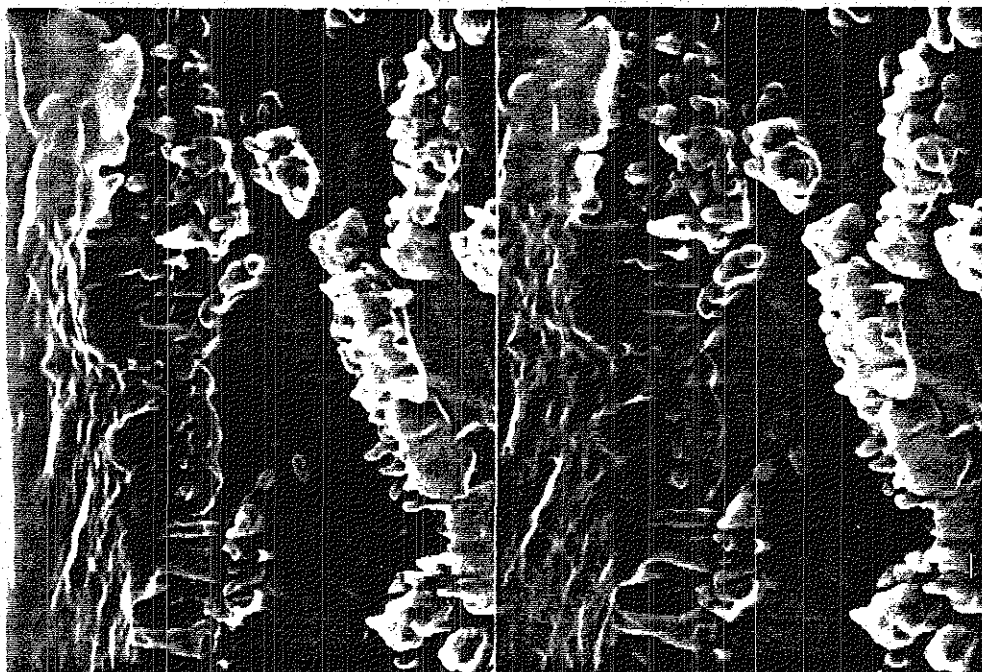
Figure 2.2.3.1-2



1.0 micrometer

10V CAA PRIMED WITH P.P.Q. - NO ENVIRONMENTAL EXPOSURE
STEREO PAIR FRACTURED VIEW SHOWING
PRIMER PENETRATION TO THE BASE OF
THE OXIDE.

Figure 2.2.3.1-3



0.5 micrometer

10V CAA PRIMED WITH P.P.Q. - NO ENVIRONMENTAL EXPOSURE
STEREO PAIR FRACTURED VIEW SHOWING
THE PRIMER PULLING AWAY FROM OXIDE.

Table 2.2.3.1-4

polymer is due to the fracturing technique used to prepare the specimens. It does show how the polymer can pull out of the oxide after penetrating the oxide to the base plate. These studies indicate that PPQ penetrates to the base of the oxide cell structure.

Polymer Thermal Analysis

Relative polymer thermal stabilities were determined by comparison of polymer glass transition temperatures before and after 10,000 hours aging at 505K (450°F). Glass transition measurements were made using Perkin-Elmer TMS-1 thermomechanical analyzer. The glass transition results are summarized in Table 2.2.3.1-1. No significant degradations were observed for any of the polymer systems, except for a slight reduction demonstrated by NR056X after aging.

2.2.3.2 Analysis of Failed Specimens

Objective

The purpose of this task is to determine the failure locus of thermally aged specimens showing strength reduction. PPQ and LARC-13 lap-shear specimens were selected for study. Thermally aged lap-shear specimens of each adhesive/surface preparation were submitted for analysis of the morphology and surface composition of the failed surfaces.

Surface Characterization Techniques

Morphology

The morphology of failed lap-shear specimens was studied both macroscopically and microscopically. Macroscopic analysis involved taking photographs at 2-3X magnifications of both surfaces of the failed bonded specimen. The microscopic morphology was studied by the STEM analysis described in Section 2.2.2.1. Micrographs were obtained at magnifications up to 100,000X. Specimens were prepared for both plan view appearance and profile view of the oxide pores. The latter specimens were prepared by the lab-fracture technique described in Section 2.2.2.1. The surface morphology seen in failed samples was then compared with the baseline

Table 2.2.3.1-1

GLASS TRANSITION TEMPERATURE OF ADHESIVES
BEFORE AND AFTER AGING AT 450°F

PPQ	557°F
PPQ Aged 10,000 Hrs	557°F
LARC-13	562°F
LARC-13 Aged 5,000 Hrs	565°F
NRO 56X	648°F
NRO 56X Aged 5,000 Hrs	562°F

studies described in Section 2.2.3.1, to enable hypotheses to be made about the crack propagation route.

Composition

The elemental surface composition of the failed lap-shear surfaces was determined by ESCA. Using this technique, the failure locus of the lap shear can be inferred to within a 100-angstrom depth over a wide area (4mm²). For example, if the elements characteristic of the adhesive—carbon, nitrogen, and oxygen—are detected by ESCA on both sides of the failed lap shear, then the failure locus is within the adhesive and/or primer layers. If titanium and oxygen are found on both surfaces, then the failure locus is within the adherend metal or oxide layer. The case where the ESCA spectra show a combination of carbon, nitrogen, oxygen, and titanium on the failed surfaces can be interpreted in two ways. First, the crack propagated alternately through the adhesive and oxide layers, leaving discrete zones of polymer and oxide on the failed surfaces. This model is shown schematically in Figure 2.2.3.2-1. The alternative interpretation is that the crack propagated along the polymer/oxide interface, leaving a uniform layer of titanium atoms less than 10 nm thick on the adhesive surface.

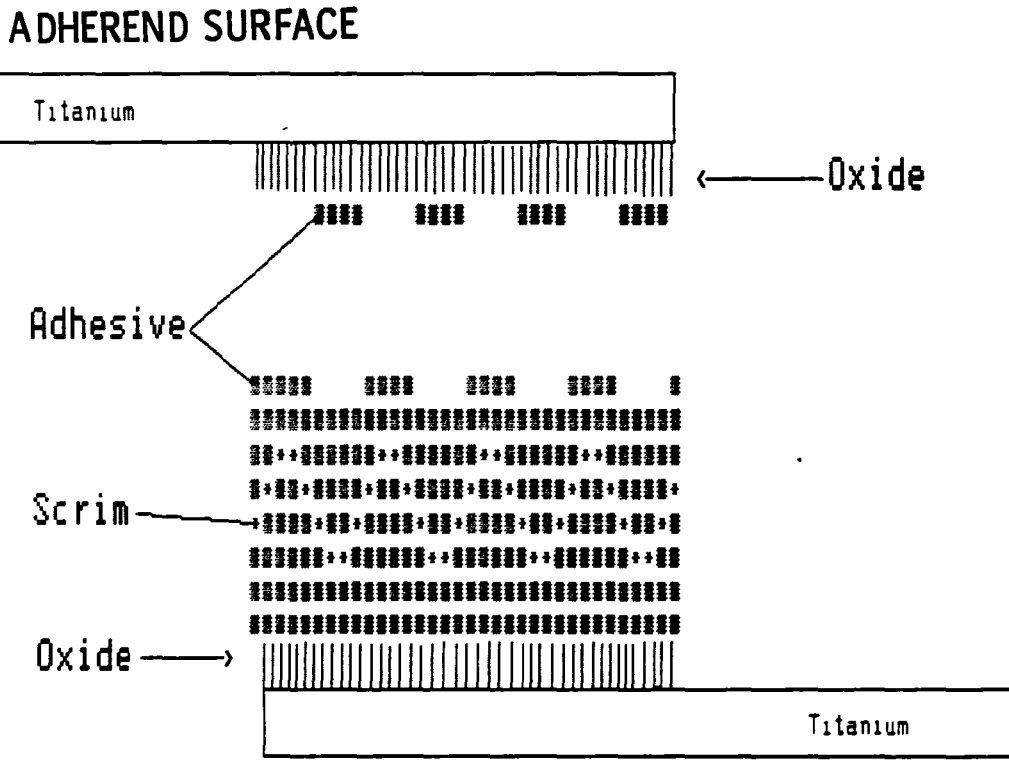
The surface chemical compositions of discrete macroscopic features identified on the adherend side of failed lap-shear specimens was determined by AES. Identification of the composition of these regions, on the adherend side, is possible because of the increased lateral resolution available with AES. Identification of polymer zones, normally a difficult task, was greatly facilitated by the closely underlying titanium substrate.

To minimize the surface contamination that usually accompanies sample handling and storage, the samples were failed by hand in the surface analysis laboratory and then analyzed immediately.

PPQ/10V CAA Lap Shear

Macroscopic Appearance

The macroscopic appearance of the PPQ/10V CAA lap shear, aged at 505K (450°F) for



SCHEMATIC LAP SHEAR FAILURE SHOWING ISLANDS OF POLYMER REMAINING ON THE OXIDE AFTER FAILURE.

Figure 2.2.3.2-1

10,000 hours, is shown in Figure 2.2.3.2-2. Both the adhesive and adherend surfaces clearly exhibit the regular woven pattern of the supporting scrim. Those areas that are light in appearance, region A, represent zones of fracture directly under the yarns of the scrim. Closer inspection of these regions reveals bright blue-green coloration on both surfaces, indicating apparent bare oxide. Those areas that are darker in appearance, region B, represent zones of fracture between the yarns of the scrim. Closer visual inspection of these regions reveals a heavy polymer coating on both the adherend and adhesive surfaces. These polymer areas do not exhibit any fracture features and appear to represent bondline porosity at the scrim nodes. This bondline porosity was found to be present in the unaged PPQ lap shears as well.

Microscopic Appearance

A plan view (Figure 2.2.3.2-3) taken from region A in figure 2.2.3.2-2 shows a thin, nonuniform layer of polymer remaining on the adherend surface. Figure 2.2.3.2-4 is a higher magnification plan view stereo pair of the same area. The details show polymer dispersed in discrete zones across an oxide layer. The 10V CAA titanium oxide layer is located in the photo by its characteristic open pore structure.

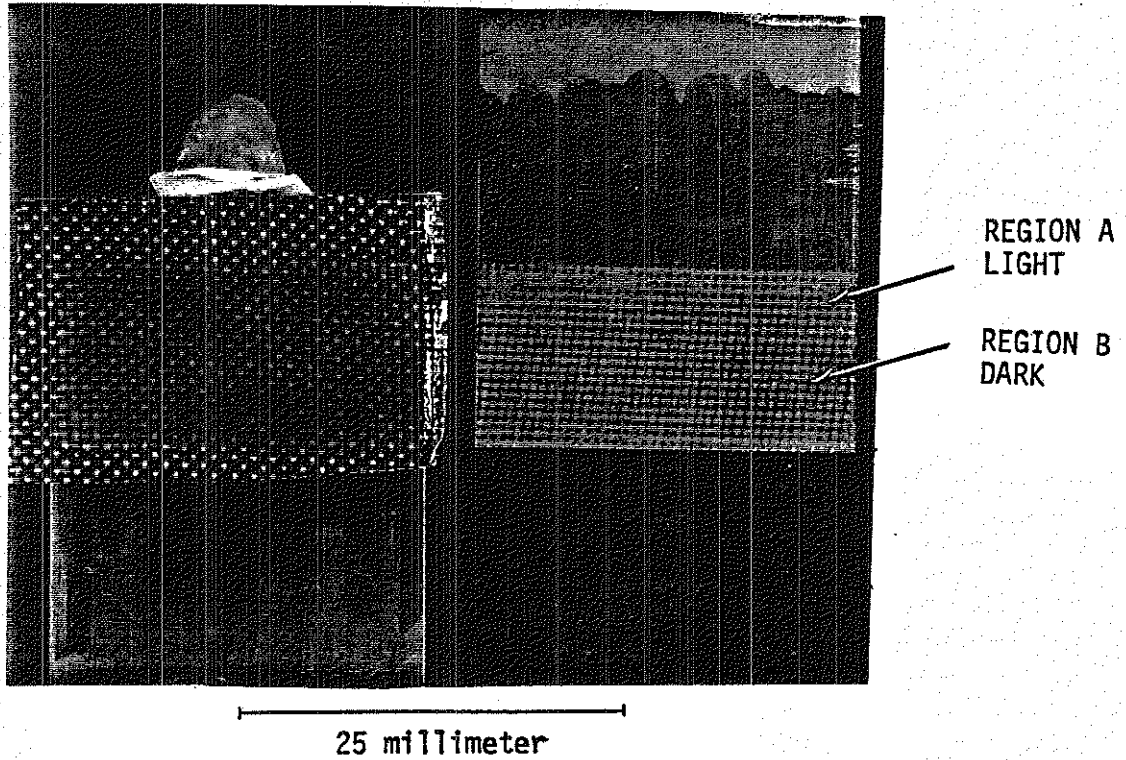
Transverse views of the adherend in region A are shown in Figures 2.2.3.2-5 and 2.2.3.2-6, after lab bend fracturing. Apparent in Figure 2.2.3.2-5 is the open side wall structure of the 10V CAA oxide. The openness of this structure suggests that no primer penetration occurred in this area. Figure 2.2.3.2-6, a stereopair of a similar area, emphasizes the overall lack of polymer penetration, except for some localized regions.

The plan view of the opposing adhesive failure surface is shown in Figure 2.2.3.2-7. The low-magnification view (Figure 2.2.3.2-7a) shows machining marks from the adherend titanium surface replicated by the polymer. At 5,000X magnification, Figure 2.2.3.2-7b shows more detail of the replicated surface. The surface undulations evident in this figure match those seen in the baseline oxide characterization (ref. Third Semi-Annual Report, May 1980, Figure 2.4.3-30b). At 50,000X magnification, Figure 2.2.3.2-7c shows a generally smooth surface morphology with depressions ~ 90 nm in diameter and small, bright nodules ~ 30 nm in diameter.

The same features are revealed in the transverse bend-fracture view shown in Figure

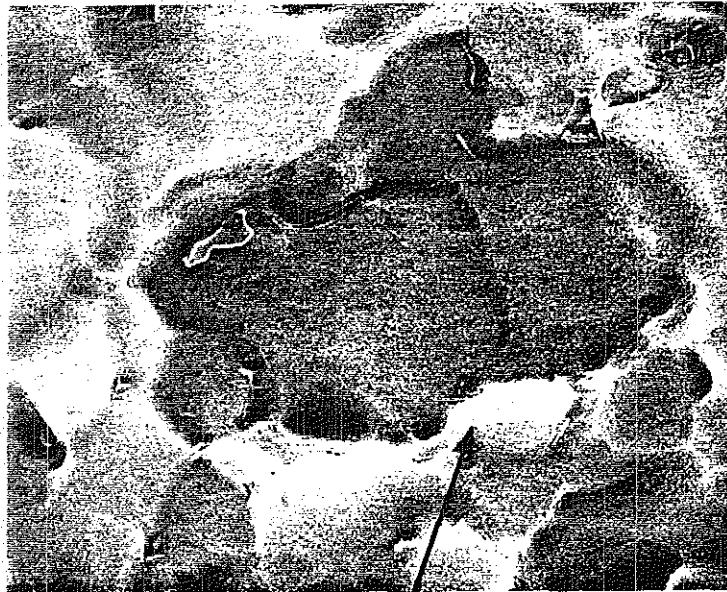
ADHESIVE

ADHEREND

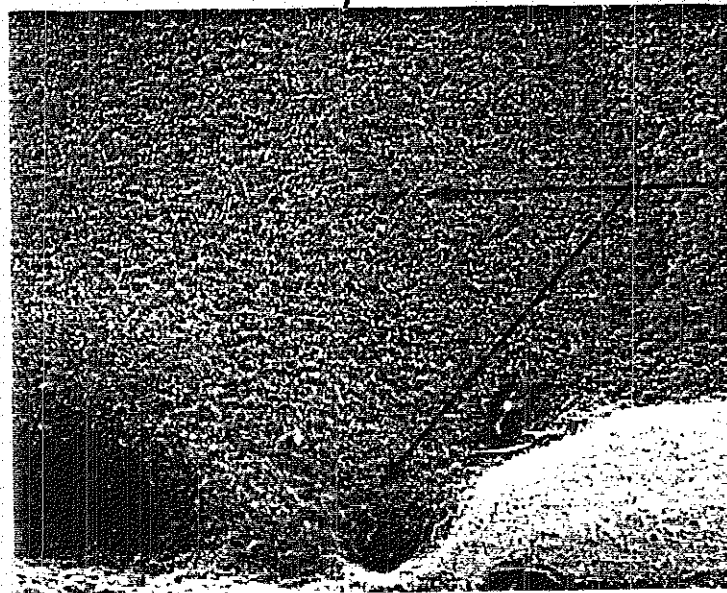


PHOTOMACROGRAPH OF FAILED PPQ/10V CAA LAP SHEAR
THERMALLY AGED AT 505°K (450°F) FOR 10,000 HOURS.

Figure 2.2.3.2-2



5.0 micrometer



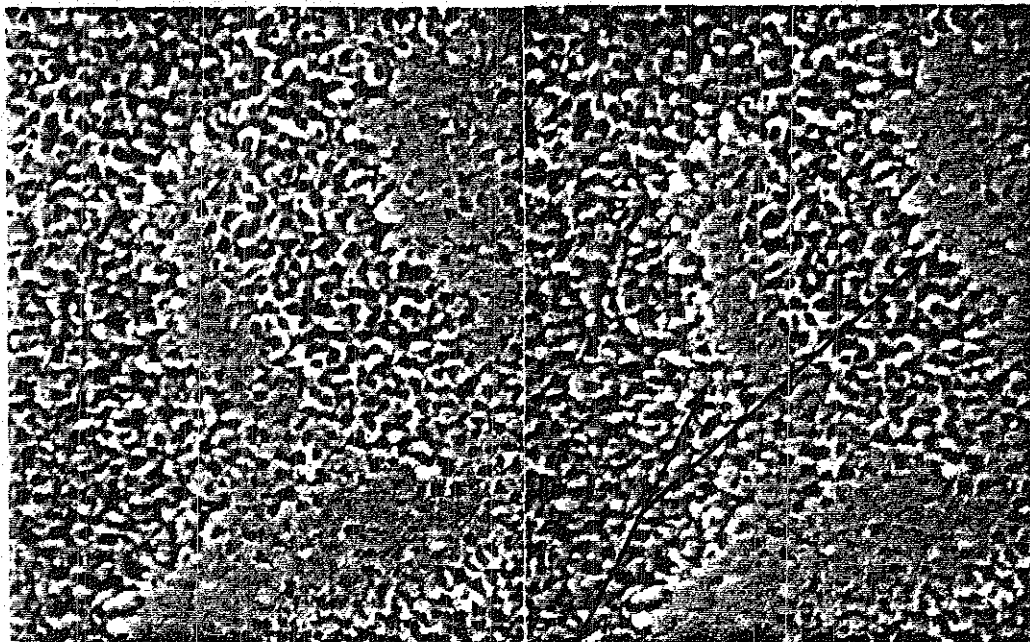
POLYMER

1.0 micrometer

10V CAA FAILED SPECIMEN - OXIDE SIDE OF FAILURE

TOP VIEW OF OXIDE FAILED SURFACE
SHOWING SOME POLYMER ON THE OXIDE
SURFACE.

Figure 2.2.3.2-3

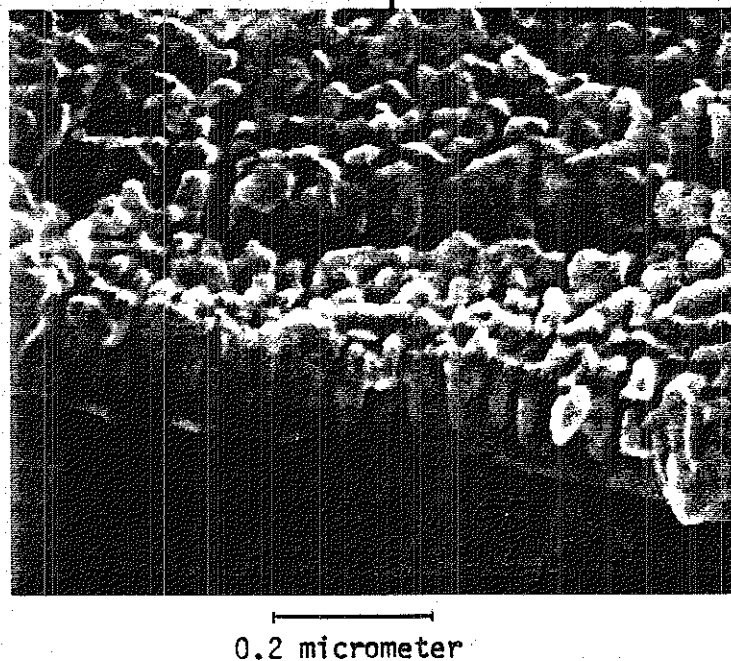
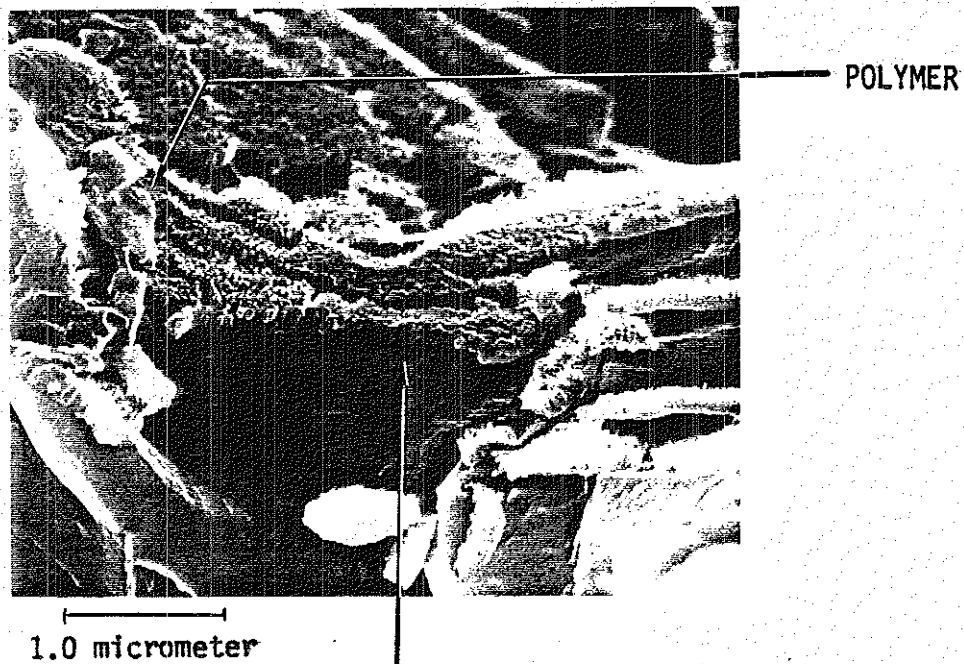


0.5 micrometer

POLYMER

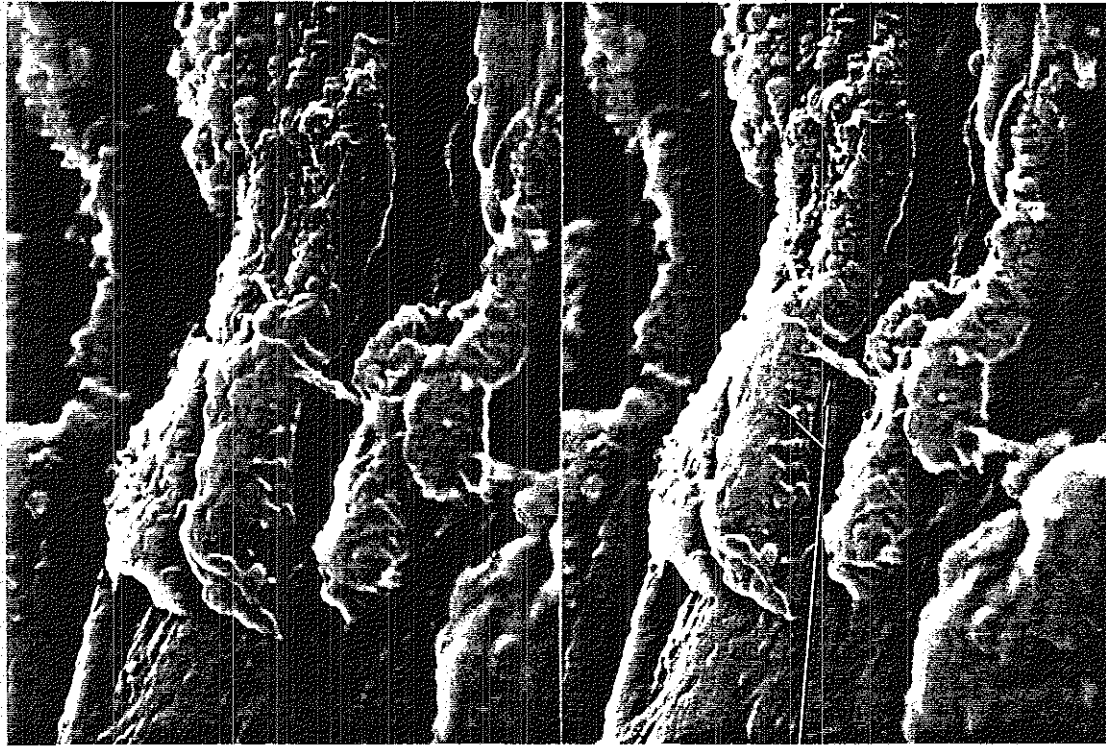
10V CAA FAILED SPECIMEN - OXIDE SIDE OF FAILURE
STEREO PAIR TOP VIEW OF OXIDE
SHOWING POLYMER ON OXIDE
(PORE SIZE ~ 30NM)

Figure 2.2.3.2-4



10V CAA FAILED SPECIMEN - OXIDE SIDE OF FAILURE
FRACTURED OXIDE OF FAILED LAP SHEAR
SPECIMEN SHOWING SOME POLYMER ON
ON OXIDE (OXIDE THICKNESS ~ 140NM)

Figure 2.2.3.2-5



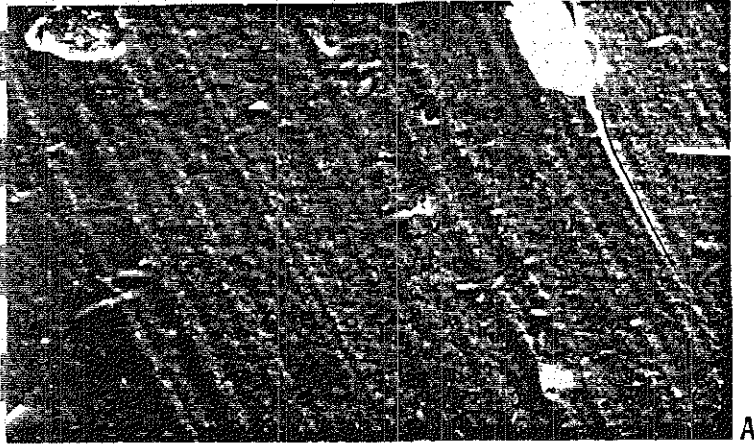
0.5 micrometer

POLYMER

10V CAA FAILED SPECIMEN - OXIDE SIDE OF FAILURE

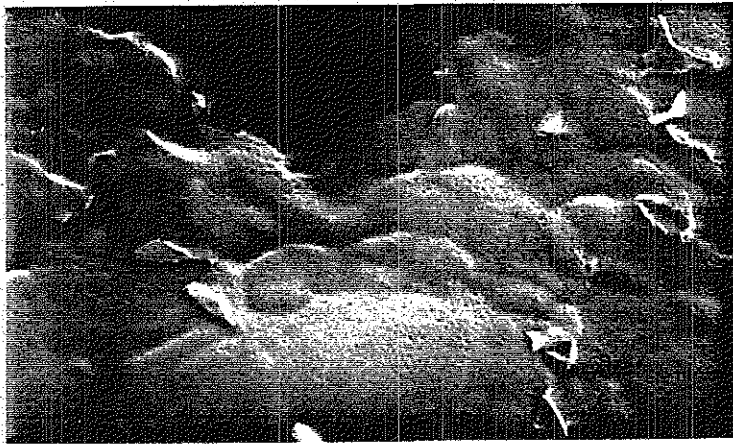
STEREO PAIR OF FRACTURED OXIDE FROM
FAILED LAP SHEAR SPECIMEN SHOWING
POLYMER ON TOP OF OXIDE, POLYMER
STRETCHING BETWEEN OXIDE ISLANDS,
AND LIMITED POLYMER PENETRATION.

Figure 2.2.3.2-6



0.2 millimeter

A



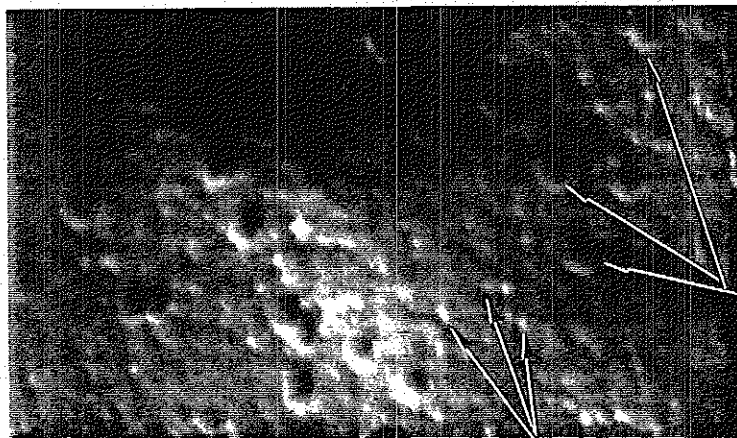
5.0 micrometer

B

10V CAA FAILED SPECIMEN - PRIMER SIDE OF FAILURE

TOP VIEW OF POLYMER SIDE OF FAILED LAP SHEAR. AT 50,000X TWO FEATURES ARE SHOWN. THESE TWO FEATURES ARE DEPRESSIONS ~ 90NM IN DIAMETER AND SMALL BRIGHT NODULES WHICH ARE ~ 30NM IN DIAMETER.

Figure 2.2.3,2-7



0.5 micrometer

C

DEPRESSIONS

NODULES

2.2.3.2-8. The size of the nodules suggests that they are formed by polymer pull-out from the oxide pores during lap-shear failure. The larger depressions, which are more evident in plan view, may be a result of polymer inhomogeneity or fracture deformation.

Surface Composition

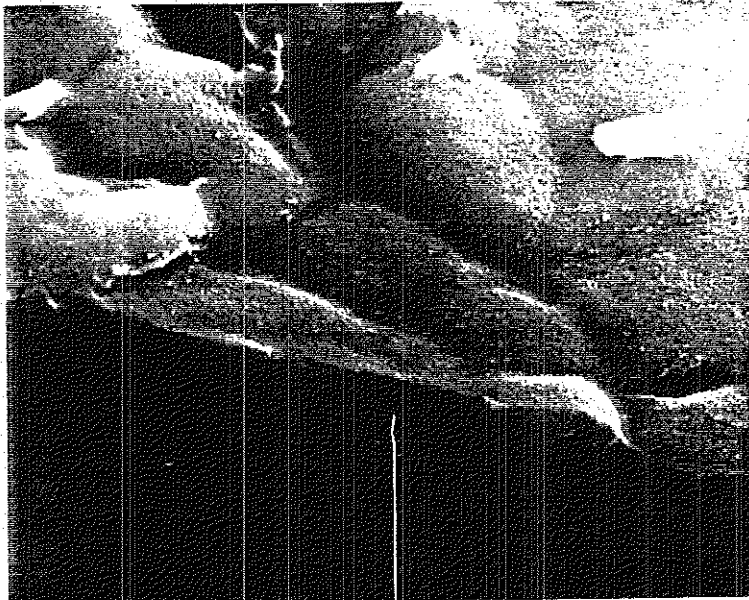
ESCA

The failed surface compositions as determined by ESCA are shown in Figures 2.2.3.2-9 and 2.2.3.2-10. The elements detected on the adhesive surface are carbon, nitrogen, oxygen, silicon, sulfur, chlorine, titanium, and lead. The adherend surface had carbon, nitrogen, oxygen, aluminum, silicon, sulfur, titanium, and lead on it. Silicon, sulfur, and chlorine are elements that are detected on most adhesive oxide fracture surfaces in varying amounts. The presence of small amounts of titanium on the adhesive surface implies that some material transfer of the titanium oxide layer occurred during failure. Also, the presence of carbon, nitrogen, and oxygen can be attributed to polymer regions B, shown in Figure 2.2.3.2-2. The resolution of this technique is not adequate to determine whether polymer transfer occurred in regions A. The presence of lead on the failed 10V CAA PPQ surface is not believed to be significant. 10V CAA LARC-13 failures have no detectable lead, yet both systems exhibit the same thermal strength degradation and failure mode.

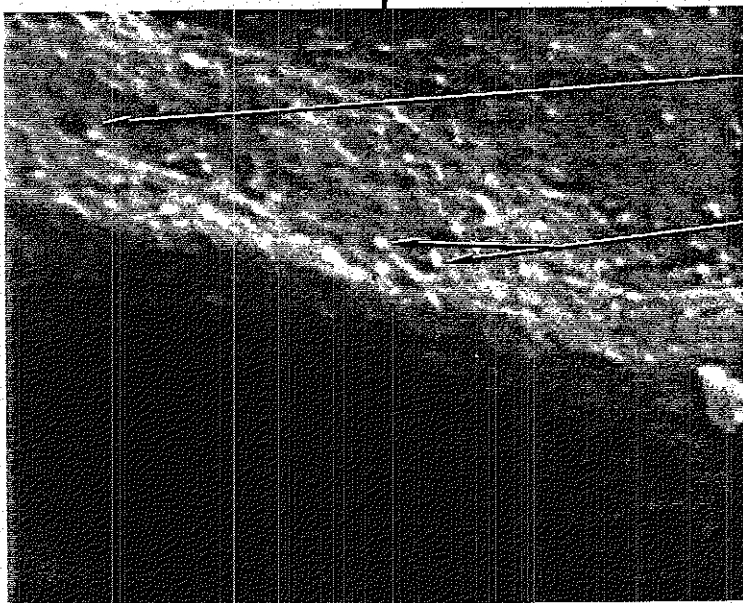
AES

AES was used for increased lateral chemical resolution of the failed adherend. Figure 2.2.3.2-11 shows an inverted absorbed-current map of a failed adherend surface at 50X shown at 2X magnification in Figure 2.2.3.2-2.

In this imaging mode, light areas correspond to areas of low conductivity and hence represent polymer. Darker areas have increased conductivity due to the presence of metal. The spectra show polymer alone (C, N, O) in region B, and a mixture of Ti oxide and polymer (C, N, O, Ti) in region A. Also identified in region A were Pb, S, and Cl. The increased lateral resolution of AES showed that the Ti oxide signal observed on the failed adherend surface by ESCA came only from the regions A.



1.0 micrometer



DEPRESSION

NODULES

0.5 micrometer

10V CAA FAILED SPECIMEN - POLYMER SIDE OF FAILURE

FRACTURED VIEW OF POLYMER SIDE OF
FAILURE ALSO SHOWS BRIGHT NODULES
AND DEPRESSIONS.

Figure 2.2.3.2-8

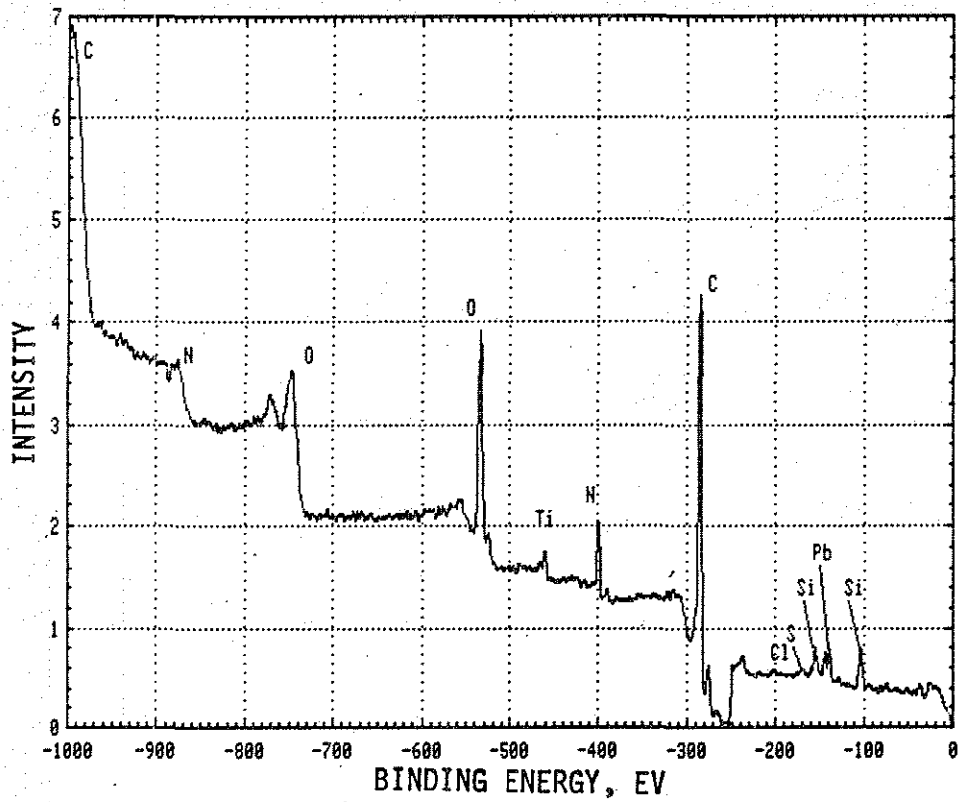


Figure 2.2.3.2-9 ESCA SPECTRUM OF THE FAILED PPQ/10V CAA LAP SHEAR, ADHESIVE SURFACE.

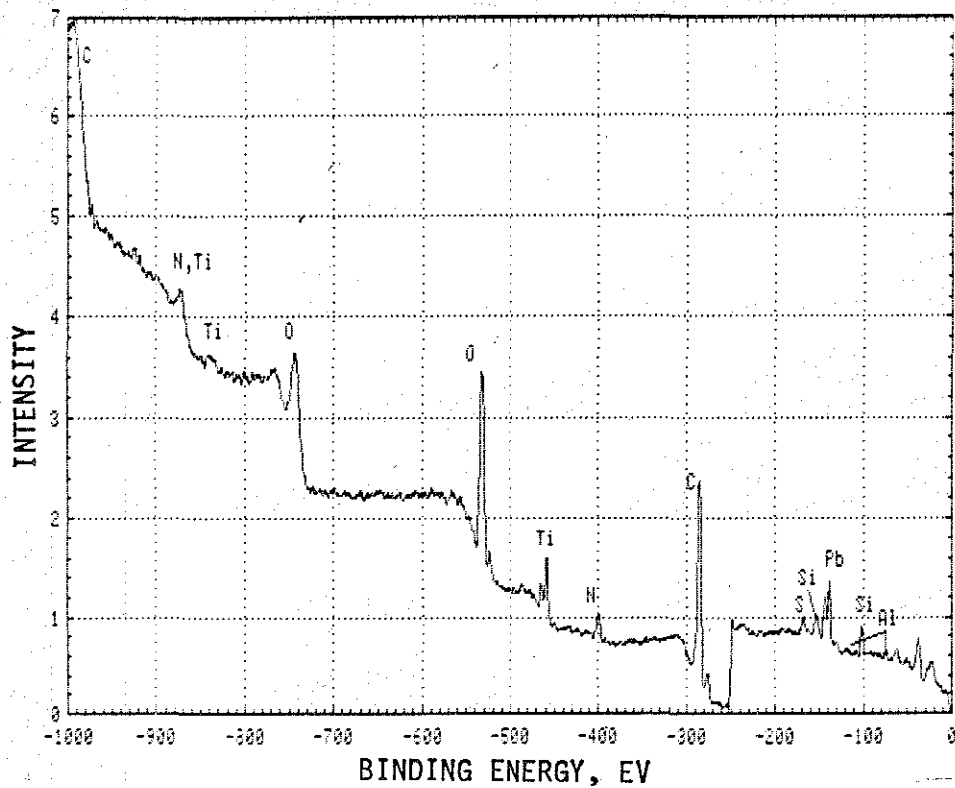
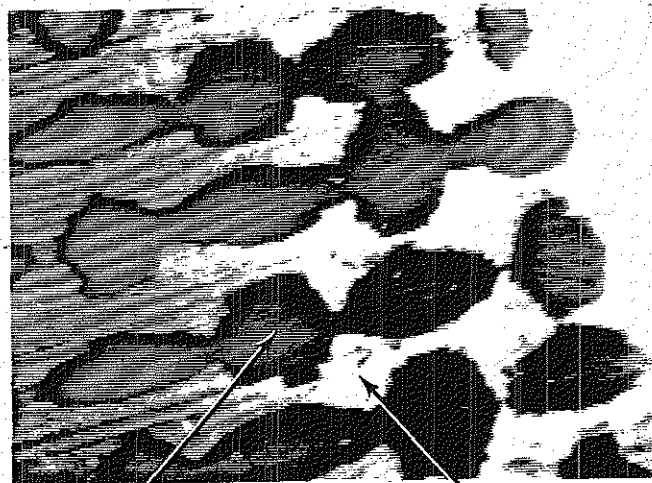


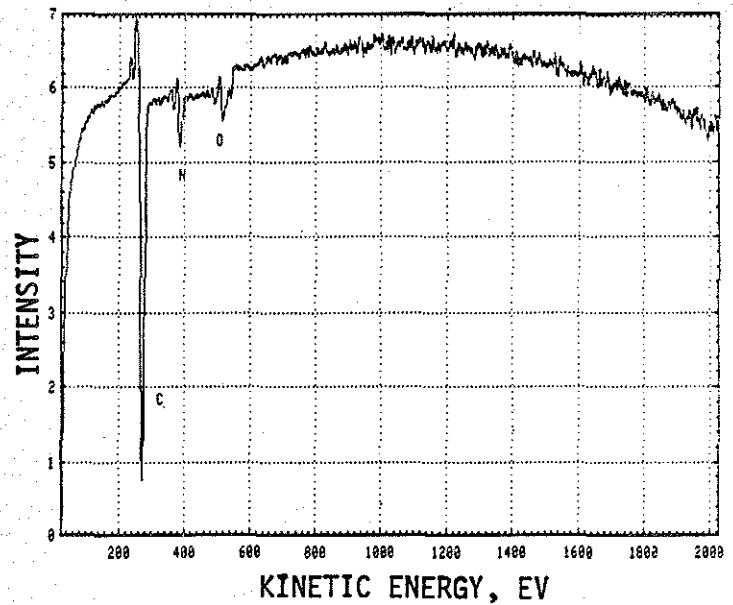
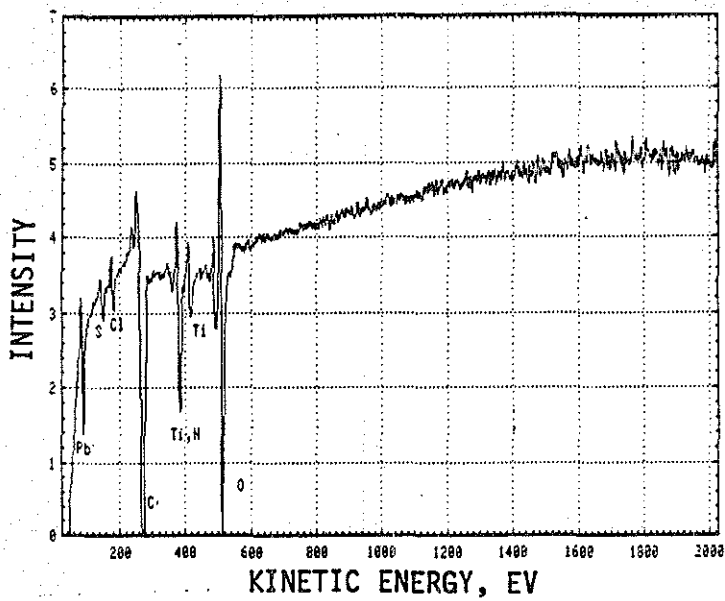
Figure 2.2.3.2-10 ESCA SPECTRUM OF THE FAILED PPQ/10V CAA LAP SHEAR, ADHEREND SURFACE.



0.5 millimeter

REGION A

REGION B



AES ANALYSIS OF REGIONS A AND B ON THE PPQ/10V CAA ADHEREND SURFACE (50X INVERTED ABSORBED CURRENT IMAGE)

Figure 2.2.3.2-11

TEM/Microtomy

The TEM/microtomy technique was used to determine if the Ti oxide signal from regions A on the adhesive side of a failure (ESCA) were due to a thin layer of oxide or to thicker, discrete areas. The Ti signal would be the same under both conditions since ESCA does not have the resolution to distinguish between the two options.

Bulk EDX in the SEM on the adhesive failed surface showed no Ti signal. A thin surface layer of Ti oxide may have been present, but below the detection limit of the bulk analysis technique. Thin sections were prepared on a microtome for EDX analysis in the STEM (transmission mode). A specimen from the failed surface was coated with a layer of Au/Pd to a thickness of ~ 30 nm to define the surface in the section. Any Ti oxide on the polymer surface would show sandwiched between the primer layer and the Au/Pd coating layer in the section. The Au/Pd layer clearly indicated the location of the failed polymer surface. No discrete areas of Ti oxide were visible in the TEM mode (Figure 2.2.3.2-12). The sectioned specimen was analyzed with EDX. No titanium was found in any of several different areas (see Figures 2.2.3.2-13 and 2.2.3.2-14). These figures show the spectra of typical areas analyzed and the elements found. The Au/Pd signals are due to the surface coating. The Cu and Mo are background signals from the instrument. No Ti signal was detected, indicating that the Ti detected by ESCA was due to a very thin Ti oxide layer spread over the polymer surface, not to discrete areas.

PPQ/5V CAA Lap Shear

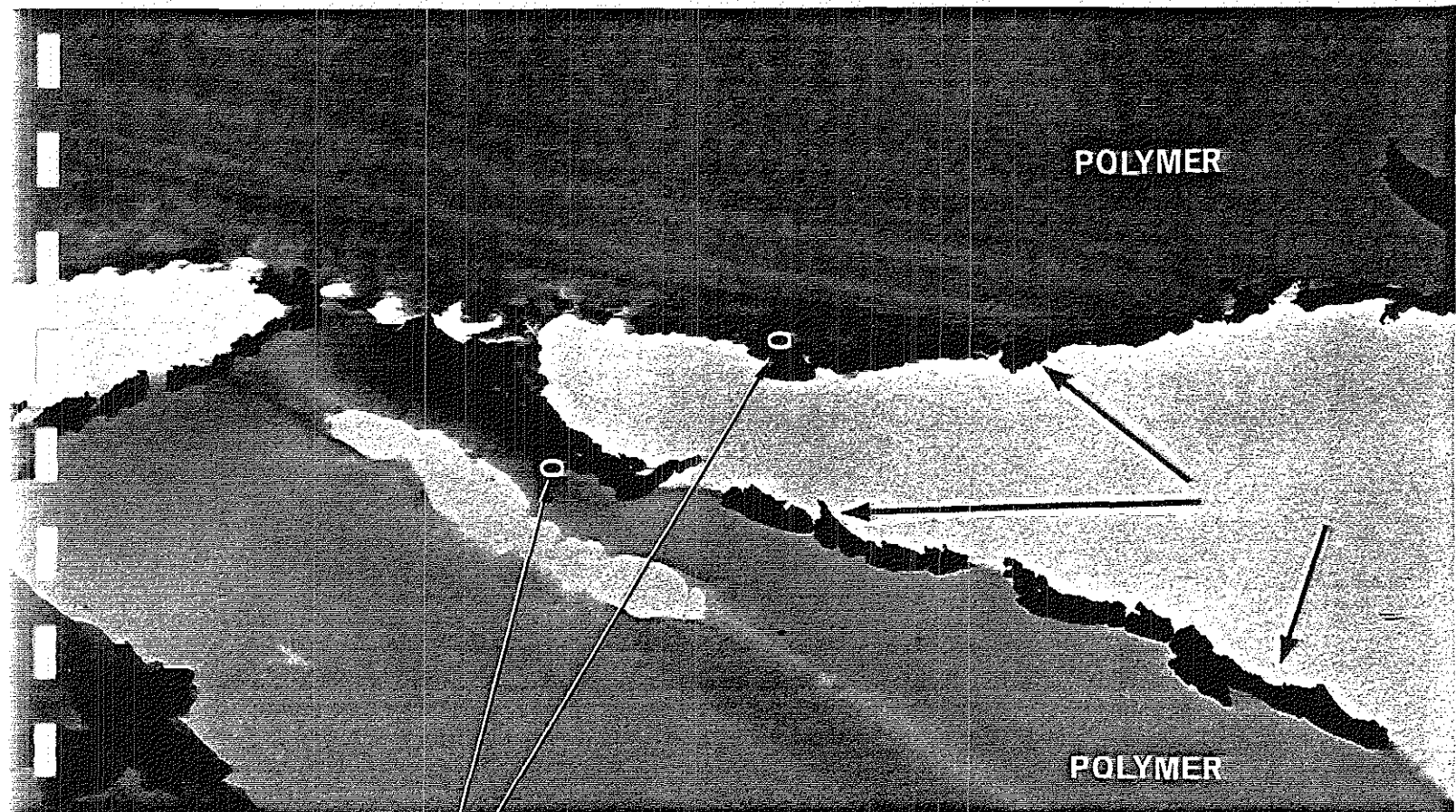
Morphology

Macroscopic Appearance

The thermally aged, failed surfaces of PPQ/5V CAA are shown in Figure ^{2.2.}3.2-15. The macroscopic appearance is identical to that of the PPQ/10V CAA lap shears.

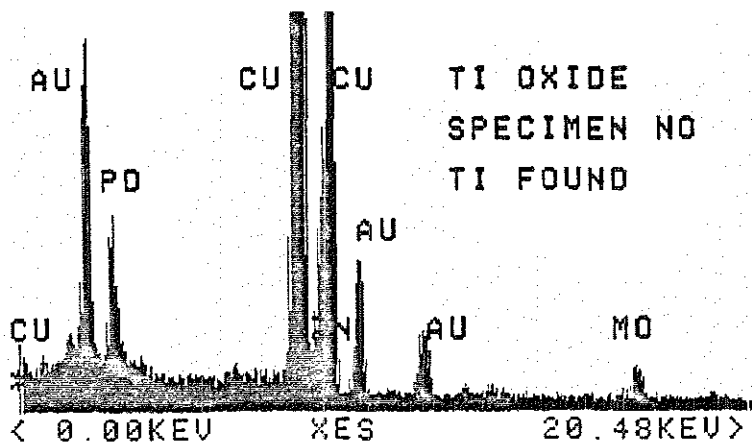
Microscopic Appearance

Low- and high-magnification plan-view micrographs of region A of the failed adherend surface are shown in Figures 2.2.3.2-16 and 2.2.3.2-17. Figure 2.2.3.2-16 shows the



0.5 micrometer

EAL2
 PR= 200S 200SEC 0 INT
 U: 1024 H=20KEV 1:30 AQ=20KEV 1Q



10V CAA FAILED SPECIMEN
 POLYMER SIDE OF FAILURE

TEM/MICROTOMY SECTION OF FAILED POLYMER
 SURFACE SHOWING TWO EDX ANALYSIS AREAS
 WITH A TYPICAL EDX SPECTRUM FROM THOSE
 TWO AREAS.

Figure 2.2.3.2-12

EDX SPECTRUM

AUGUST 27, 1981

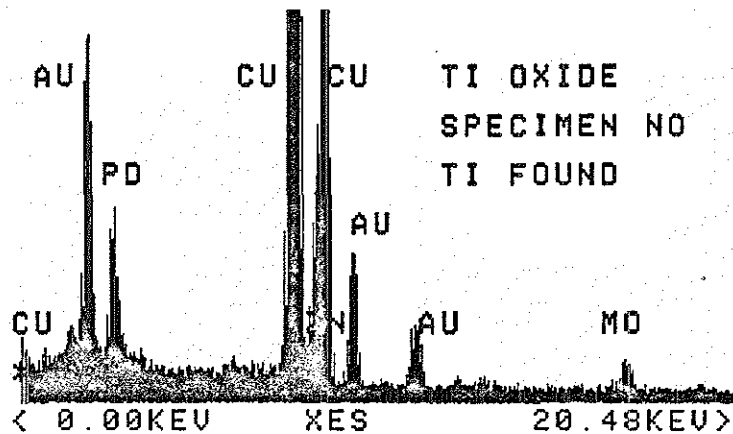
SPECTRUM EAL2

ENERGY	COUNTS	X-RAY LINES
1.65	406.	AU MZ2, AU MZ1
2.14	6783.	AU MA1, AU MA2, AU MB
2.83	2638.	PD LA1, PD LA2, AU MD, AU MIN
8.01	107917.	CU KA1, CU KA2
8.57	728.	ZN KA2
8.87	15025.	CU KB1
9.67	2602.	ZN KB2, AU LA1, AU LA2
11.45	1071.	AU LB1
17.39	484.	MO KA2

EAL2

PR= 200S 200SEC 0 INT

V= 1024 H=20KEV 1:30 AQ=20KEV 10



EDX SPECTRUM

10V CAA FAILED SPECIMEN - POLYMER SIDE OF FAILURE

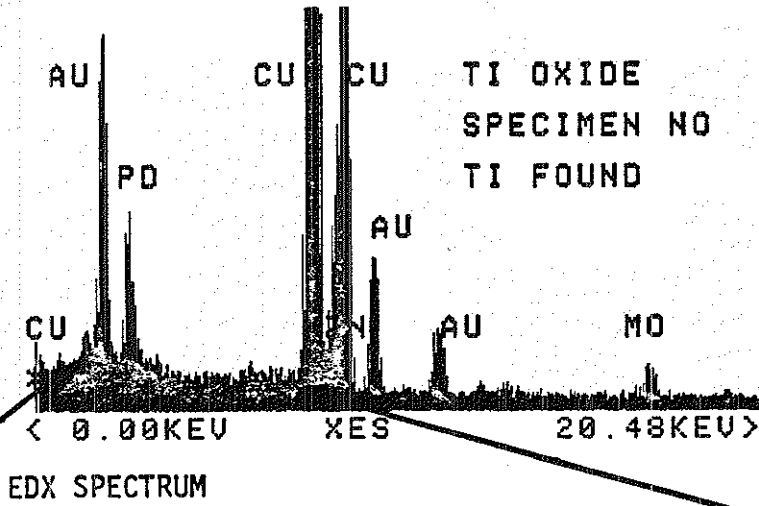
PRINTOUT OF EDX SPECTRUM

Figure 2.2.3.2-13

EAL2

PR= 200S 200SEC 0 INT

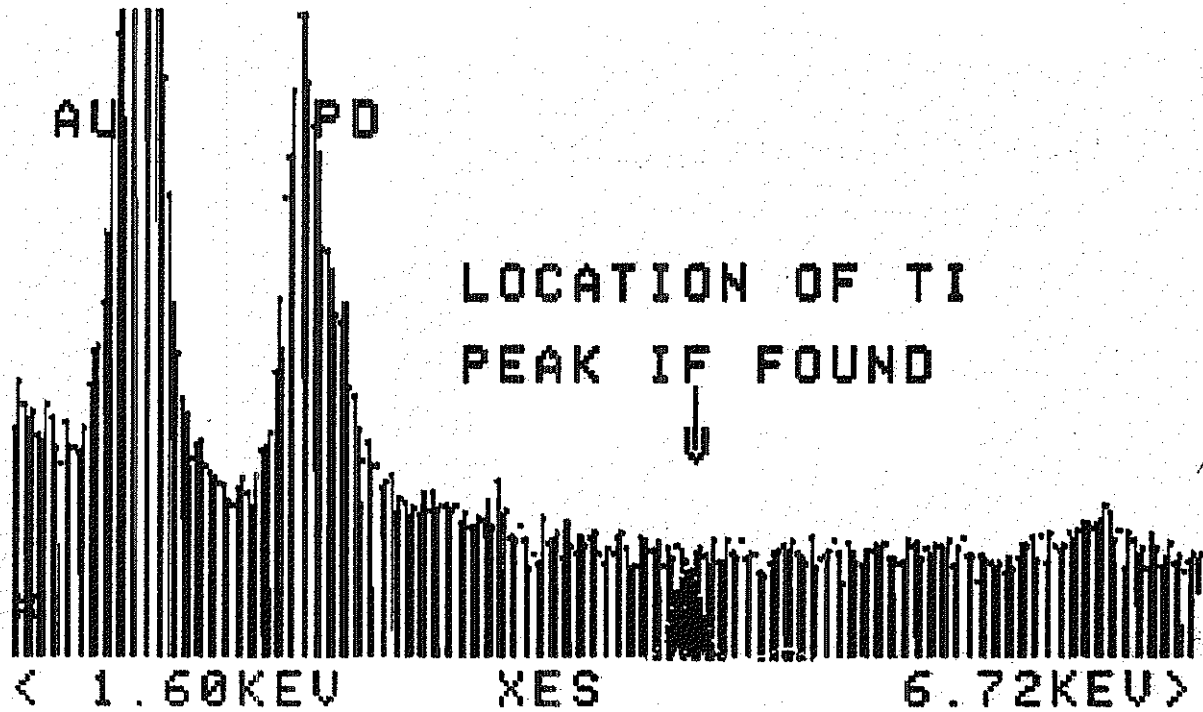
U: 1024 H=20KEV 1:30 AQ=20KEV 1Q



EAL2

PR= 200S 200SEC 0 INT

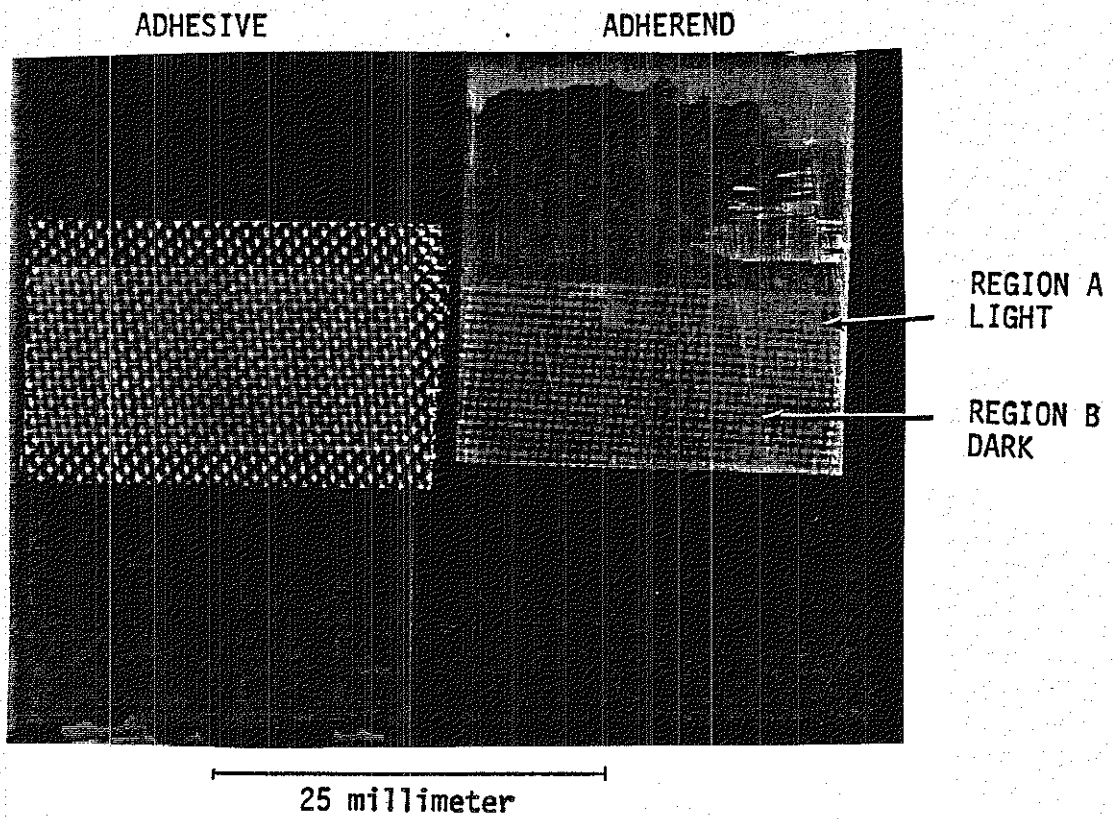
U=512 H=20KEV 1:40 AQ=20KEV 1Q



10V CAA FAILED SPECIMEN - POLYMER SIDE OF FAILURE

EDX SPECTRUM EXPANDED

Figure 2.2.3.2-14

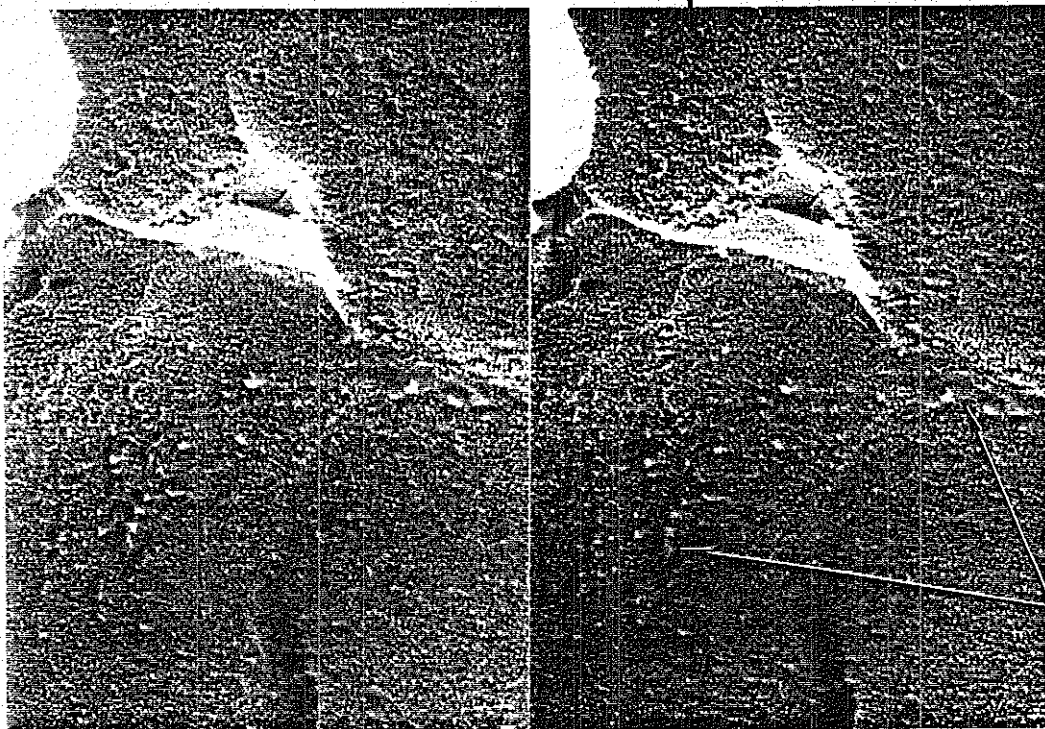


PHOTOMACROGRAPH OF FAILED PPQ/5V CAA LAP SHEAR
THERMALLY AGED AT 505⁰K (450⁰F) FOR 10,000 HOURS.

Figure 2.2.3.2-15



5.0 micrometer



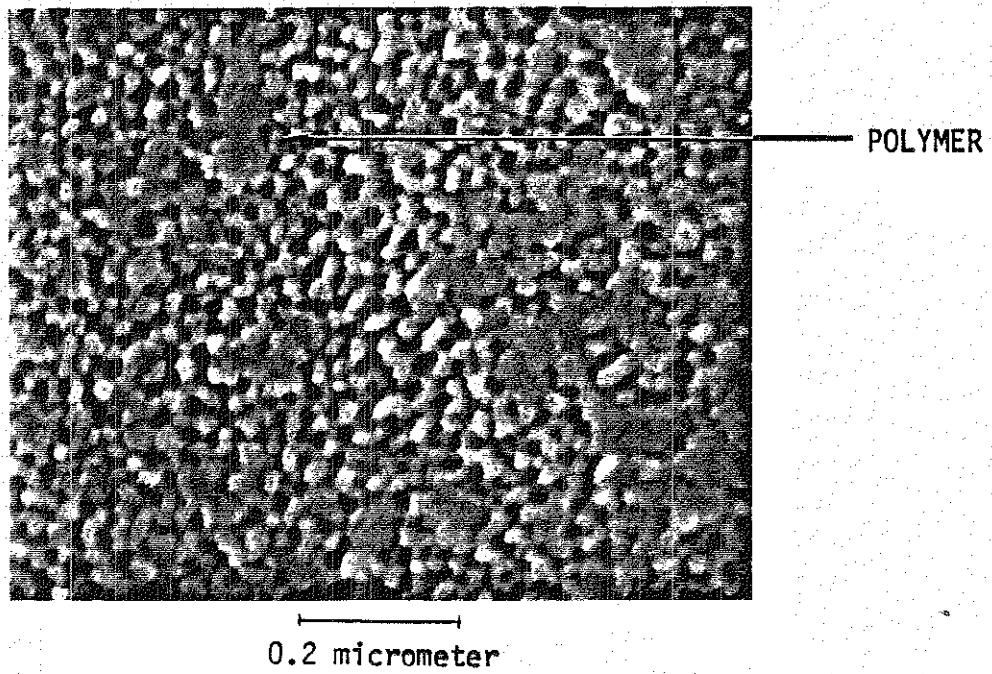
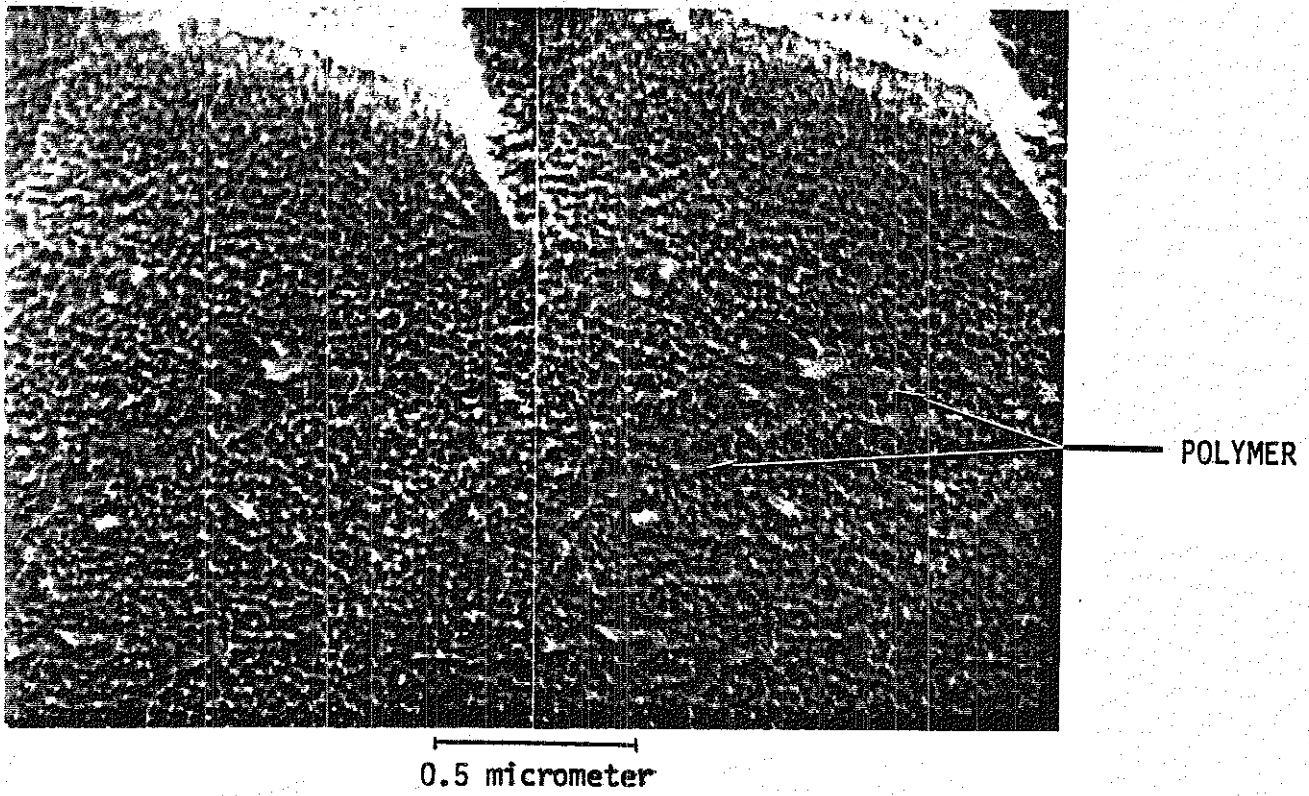
POLYMER

1.0 micrometer

5V CAA TEST FAILURE-OXIDE SIDE

STEREO PAIR SHOWING TOP VIEW OF OXIDE WITH
INDICATIONS OF THE PRESENCE OF SOME POLYMER

Figure 2.2.3.2-16



5V CAA TEST FAILURE-OXIDE SIDE

Figure 2.2.3.2-17

open pore structure characteristic of CAA Ti oxides. Figure 2.2.3.2-17, a higher magnification view of the same area, reveals the pore structure more clearly, as well as isolated areas of a thin film of polymer adhering to the surface.

Bend-fracture specimens of the same region are shown in Figure 2.2.3.2-18. The open-cell, columnar structure typical of CAA oxides is clearly revealed in these micrographs. This open structure indicates lack of polymer penetration. However, small regions of polymer adhering to the surface are visible.

Surface Composition

ESCA

ESCA spectra of adhesive and adherend surfaces of the failed PPQ 5V CAA lap shear are shown in Figures 2.2.3.2-19 and 2.2.3.2-20. The adhesive surface (Figure 2.2.3.2-19) showed carbon, nitrogen, oxygen, aluminum, silicon, titanium, and lead. The adherend surface composition (Figure 2.2.3.2-20) was carbon, nitrogen, oxygen, aluminum, titanium, and lead. As for PPQ 10V CAA, the presence of titanium on the adhesive surface implies that some material transfer of the Ti oxide layer occurred during failure. Carbon, nitrogen, and oxygen on the adherend surface can be attributed to polymer regions B shown in Figure 2.2.3.2-15. The resolution of ESCA is not adequate to determine whether polymer transfer occurred in regions A.

AES

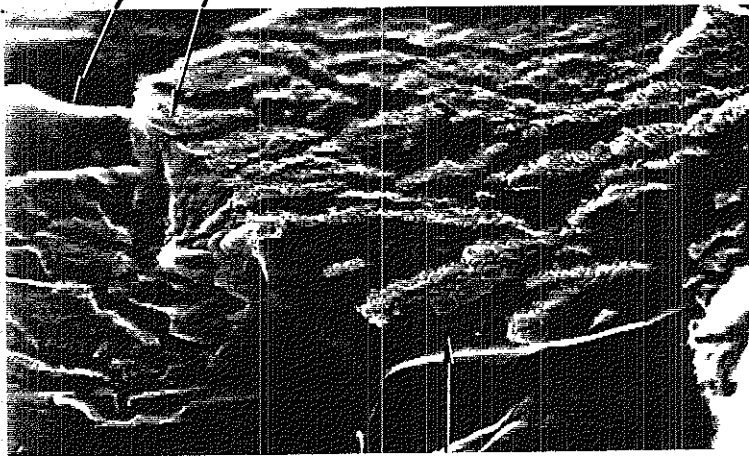
An inverted absorbed-current image of the failed adherend surface is shown in Figure 2.2.3.2-21 at 50X magnification, together with AES spectra for regions A and B. As for PPQ/10V CAA, region B consisted of polymer alone, whereas region A showed Ti oxide with polymer. Anomalous to the ESCA data on the adherend surface, lead was not detected by AES.

LARC-13/10V CAA Lap Shear

Morphology

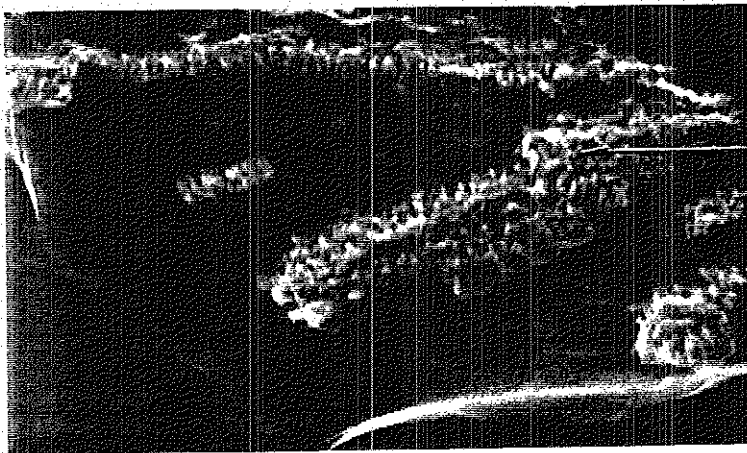
Macroscopic Appearance

POLYMER



1.0 micrometer

POLYMER

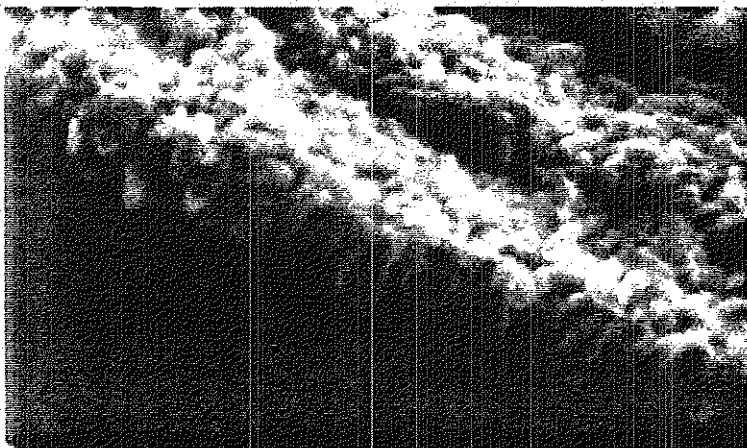


0.5 micrometer

5V CAA TEST FAILURE-OXIDE SIDE

FRACTURED OXIDE WITH VERY SMALL AMOUNTS OF POLYMER PRESENT AND AN OXIDE THICKNESS OF ~130NM.

Figure 2.2.3.2-18



0.2 micrometer

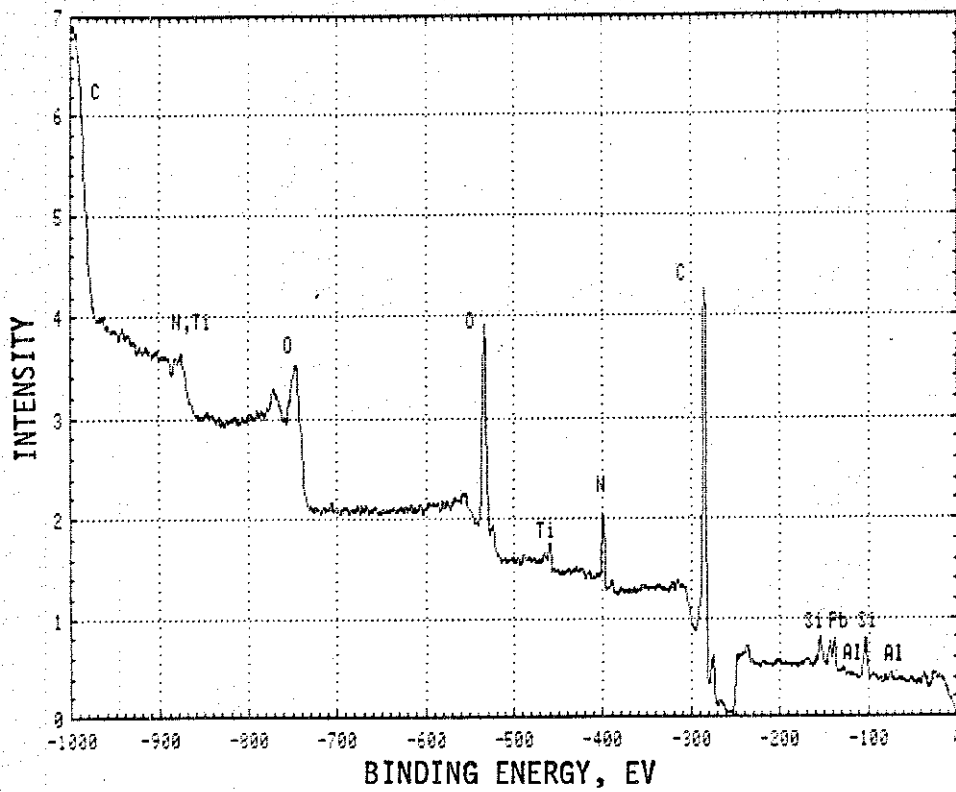


Figure 2.2.3.2-19 ESCA SPECTRUM OF THE FAILED PPQ/5V CAA LAP SHEAR, ADHESIVE SURFACE.

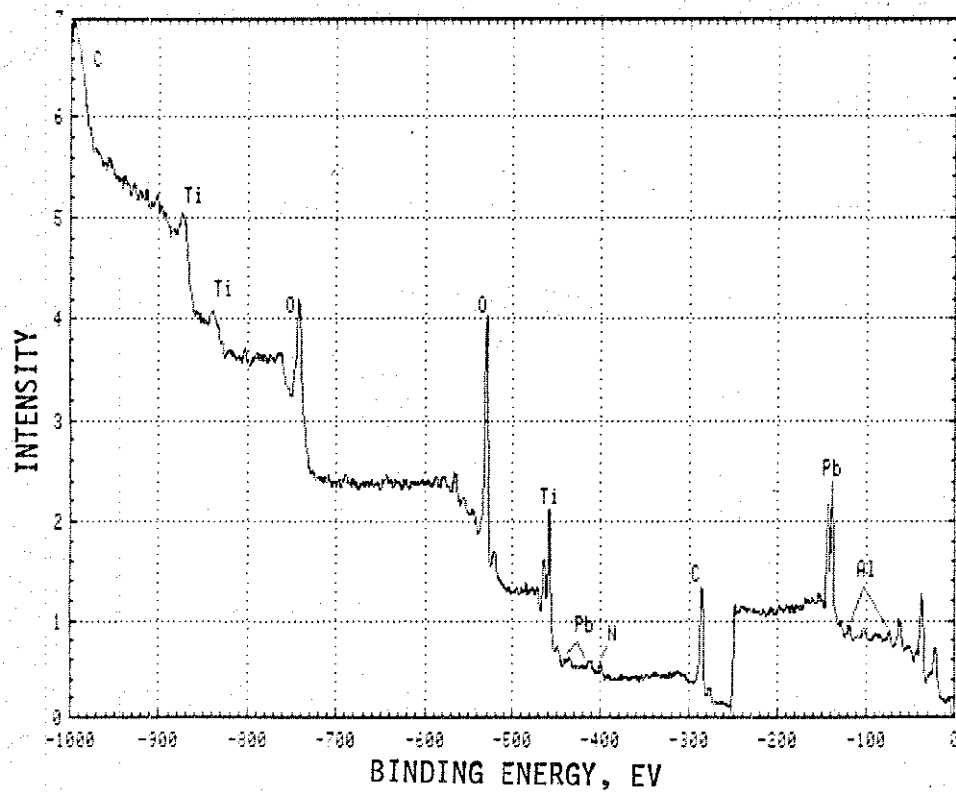
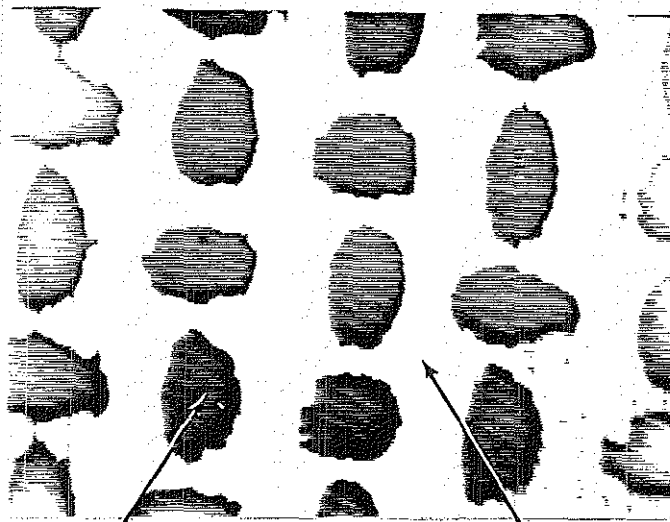


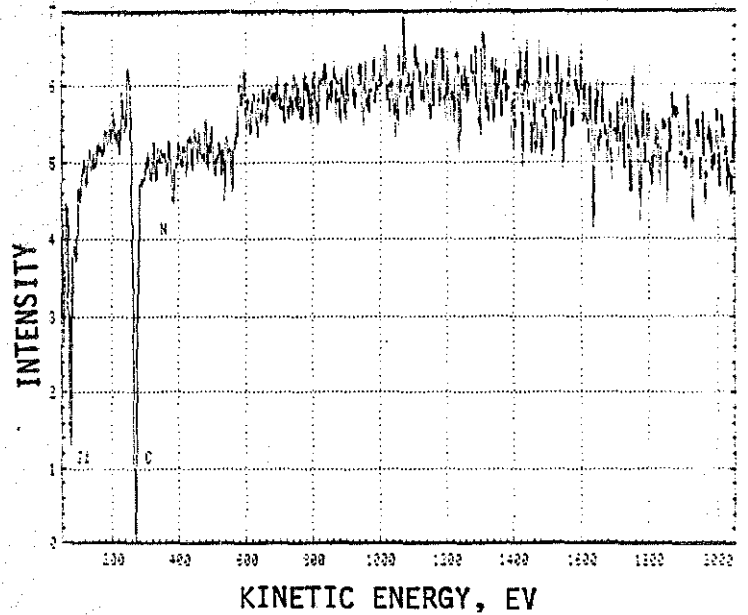
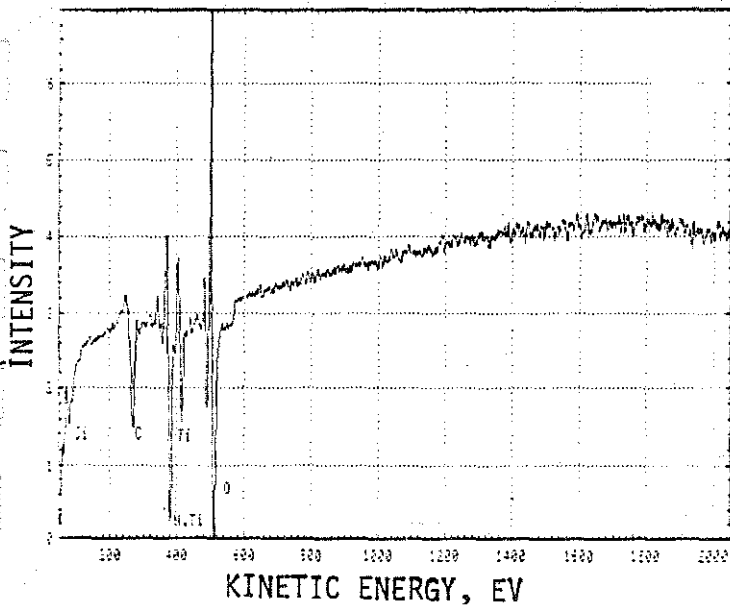
Figure 2.2.3.2-20 ESCA SPECTRUM OF THE FAILED PPQ/5V CAA LAP SHEAR, ADHEREND SURFACE



0.5 millimeter

REGION A

REGION B



AES ANALYSIS OF REGIONS A AND B ON THE PPQ/5V CAA ADHEREND SURFACE (50X INVERTED ABSORBED CURRENT IMAGE).

Figure 2.2.3.2-21

The macroscopic appearance of failed 10,000-hour, 505K (450°F), LARC-13, 10V CAA lap shears is shown in Figure 2.2.3.2-22. The appearance contrasts sharply with that of PPQ lap-shear failures.

Extended areas on both adherend surfaces appear to be predominantly exposed oxides, with exposed areas of polymer on the mating surfaces, the adhesive polymer flaking away from both surfaces. Also evident is a high degree of porosity at the scrim nodes. The white borders are due to segregation of aluminum filler particles.

Both the segregation of Al filler particles and scrim node porosity were also observed in unaged samples.

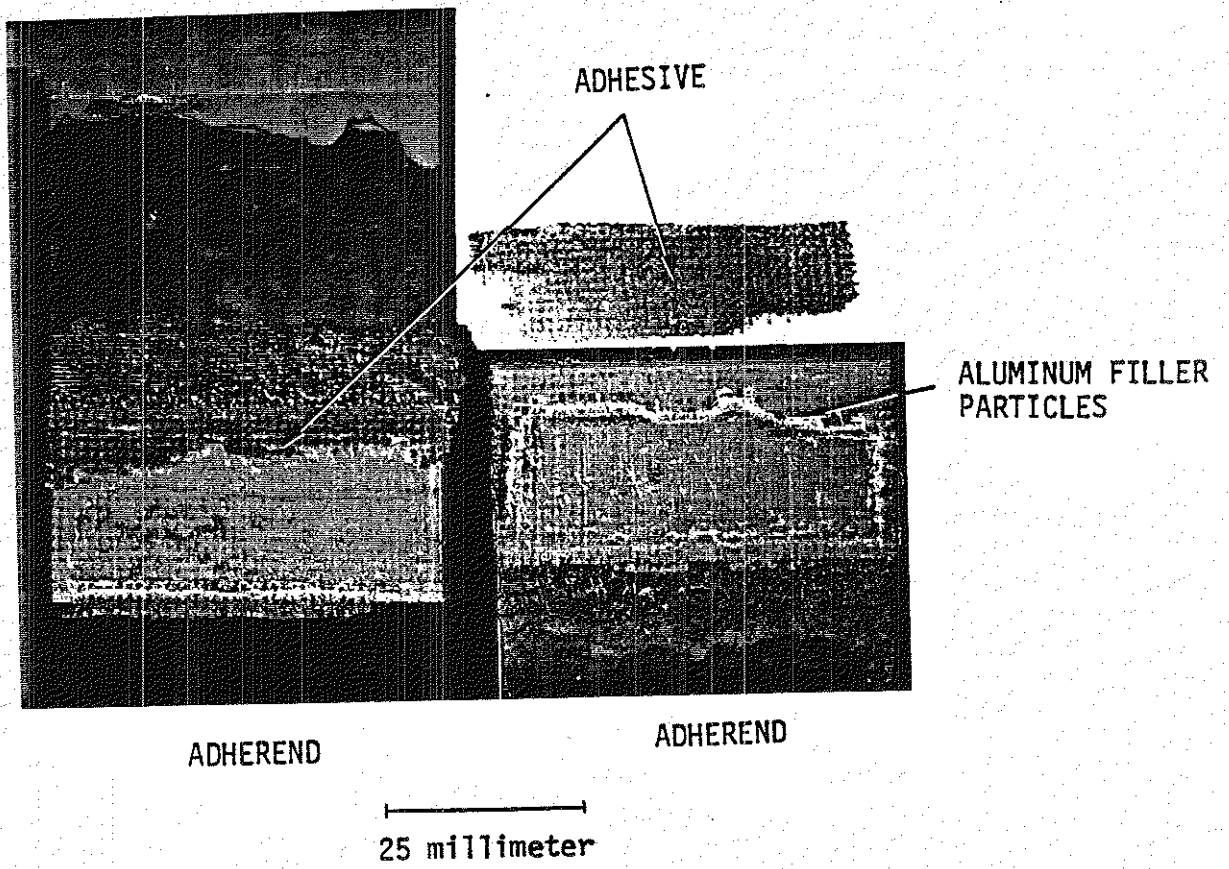
Microscopic Appearance

The failed adherend surface, shown in Figure 2.2.3.2-23, has distinct thick regions of polymer adhering to the oxide layer. There are also large areas of exposed oxide. Figure 2.2.3.2-24 is a high magnification view of the region indicated in Figure 2.2.3.2-23b.

Evident at this magnification (Figure 2.2.3.2-24b) is the typical open cell structure of 10V CAA. Figure 2.2.3.2-24a shows the gradually diminishing polymer adhesion with distance from thick polymer zones. Figure 2.2.3.2-25 is a bend-fractured view of the adherend in a polymer/oxide transition zone. The higher magnification view reveals the open columnar structure of the oxide adjacent to a thick polymer layer. As with previous 10V CAA studies, there is no evident primer penetration into the oxide.

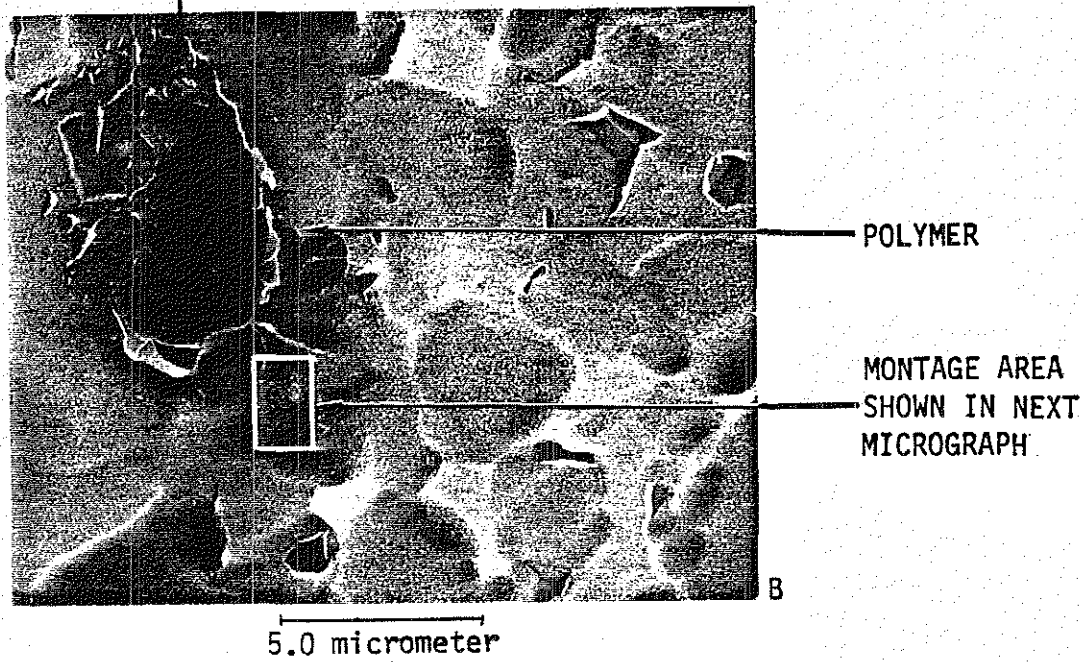
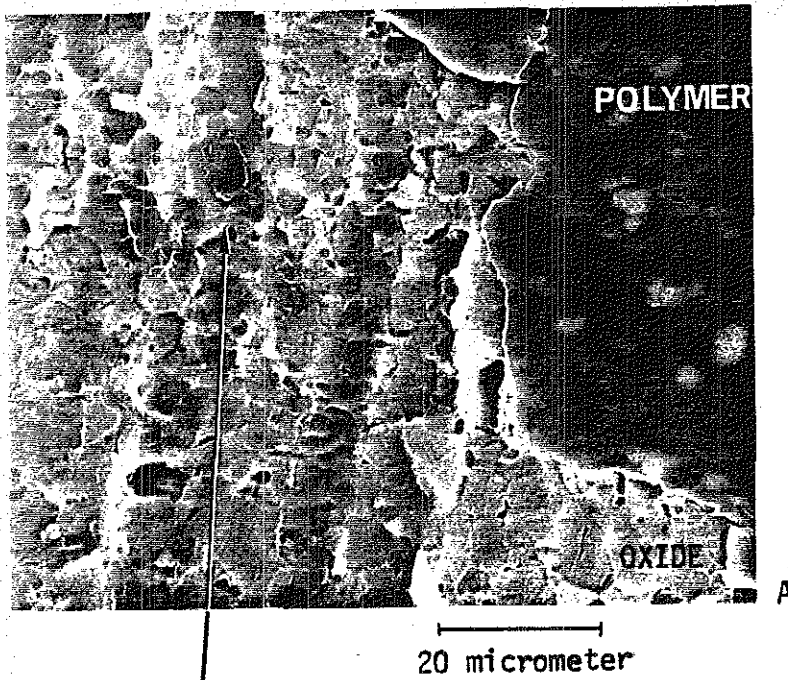
A stereographic fracture view of the adherend in an area well away from the polymer is shown in Figure 2.2.3.2-26. No polymer adhesion or penetration into the oxide structure is evident.

The adhesive side of the failure surface is shown in Figure 2.2.3.2-27. This surface has the replicated appearance of the adherend layer. At lower magnifications (Figure 2.2.3.2-27a), the replication shows machining grooves of the Ti surface. Figure 2.2.3.2-27b at higher magnifications, reveals the replication of the undulating oxide morphology. Both figures show a dispersion of small, light particles within the



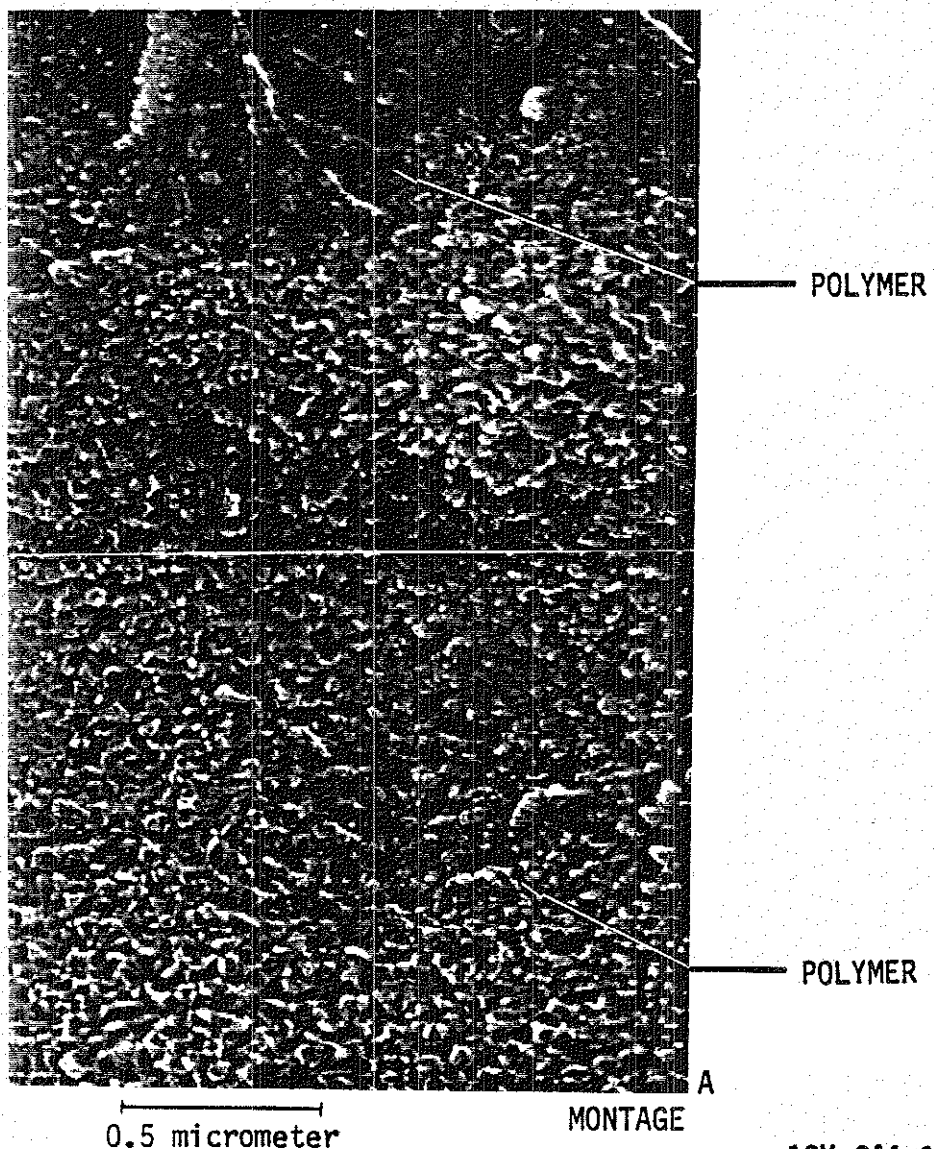
PHOTOMICROGRAPH OF FAILED LARC-13/10V CAA LAP SHEAR
THERMALLY AGED AT 505°K (450°F) FOR 10,000 HOURS.

Figure 2.2.3.2-22



10V CAA 10,000 HOURS TEST FAILURE-OXIDE SIDE
 TOP VIEW OF TEST FAILURE SHOWING
 POLYMER ISLANDS ON TOP OF OXIDE
 SURFACE.

Figure 2.2.3.2-23



10V CAA 10,000 HOURS TEST FAILURE-OXIDE SIDE

TOP VIEW SHOWING SOME POLYMER
 ATOP ESSENTIALLY OPEN-CELLED OXIDE
 (PORE SIZE 30NM IN DIAMETER)

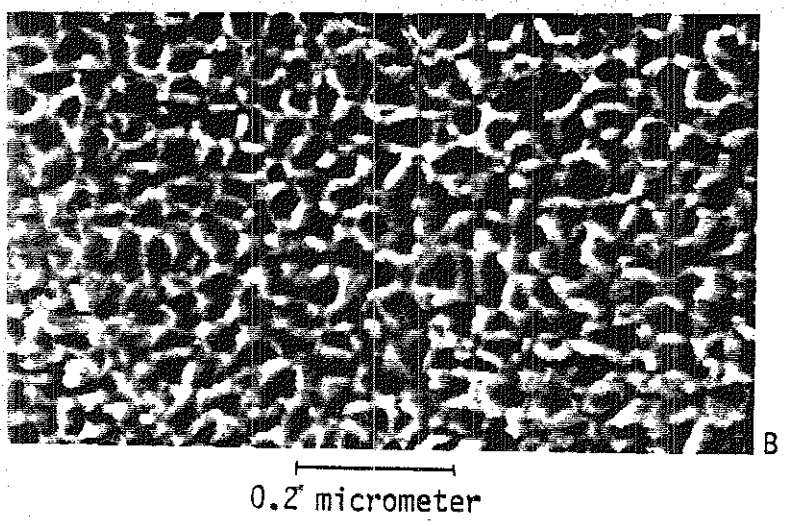
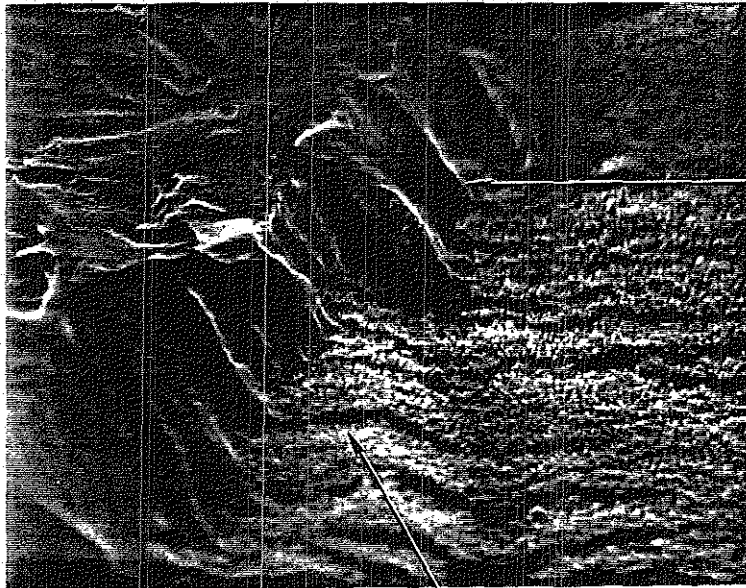
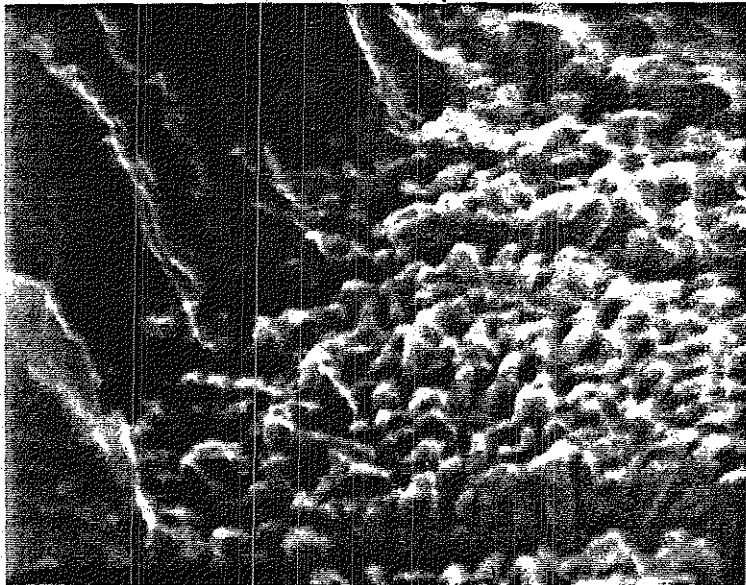


Figure 2.2.3.2-24



POLYMER

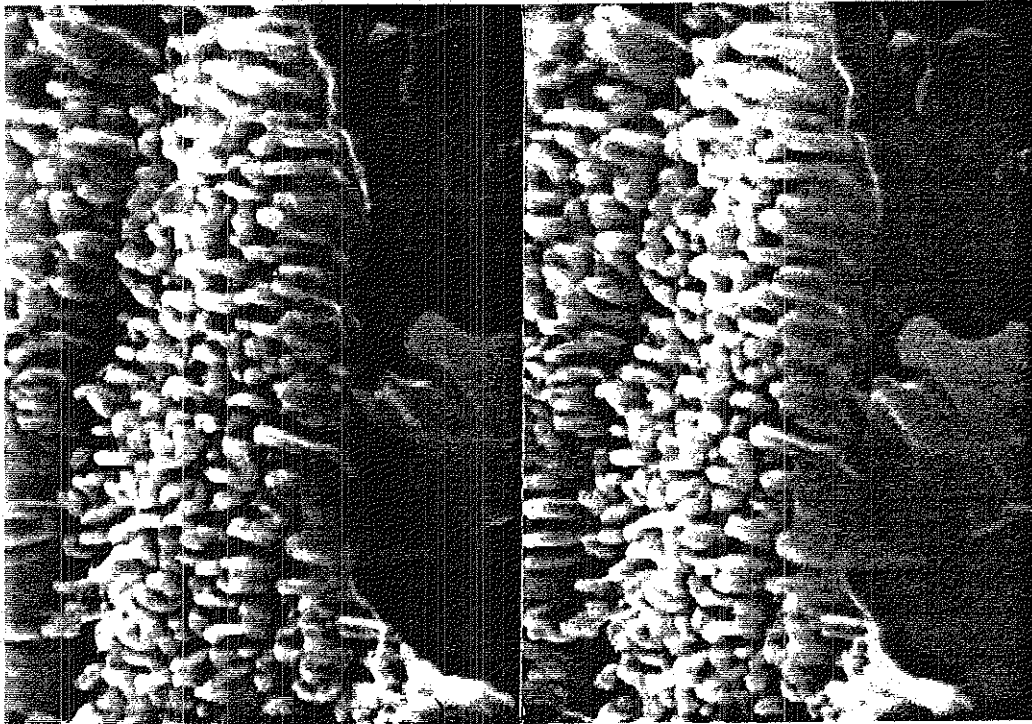
1.0 micrometer



0.2 micrometer

10V CAA 10,000 HOURS TEST FAILURE-OXIDE SIDE
POLYMER/OXIDE INTERFACE SHOWN
IN LAB-FRACTURED VIEWS

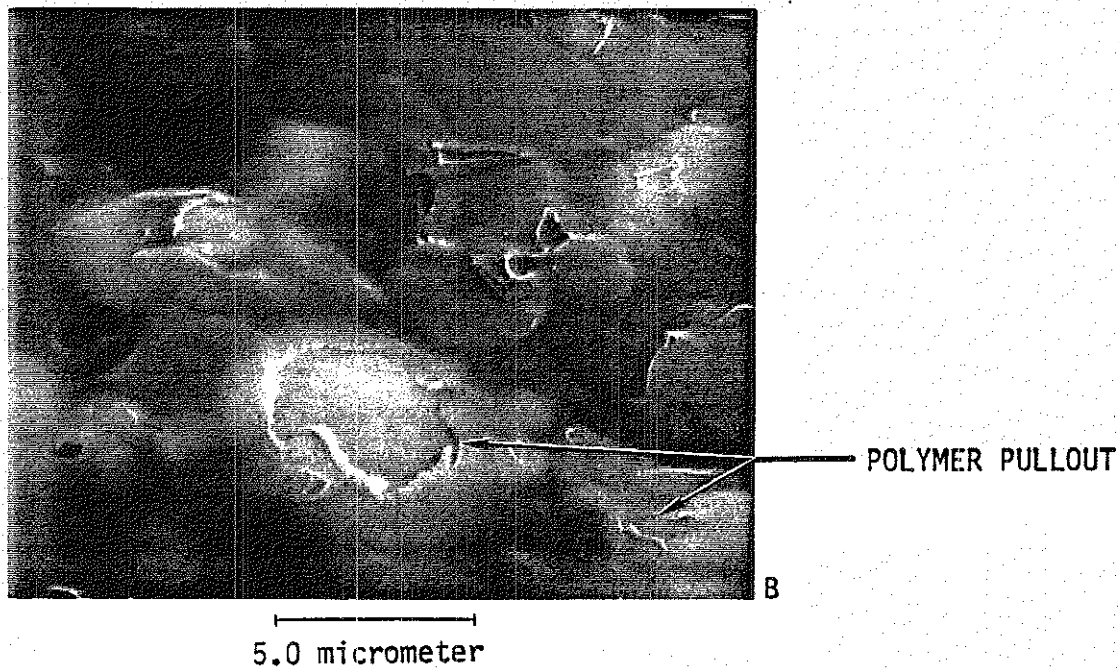
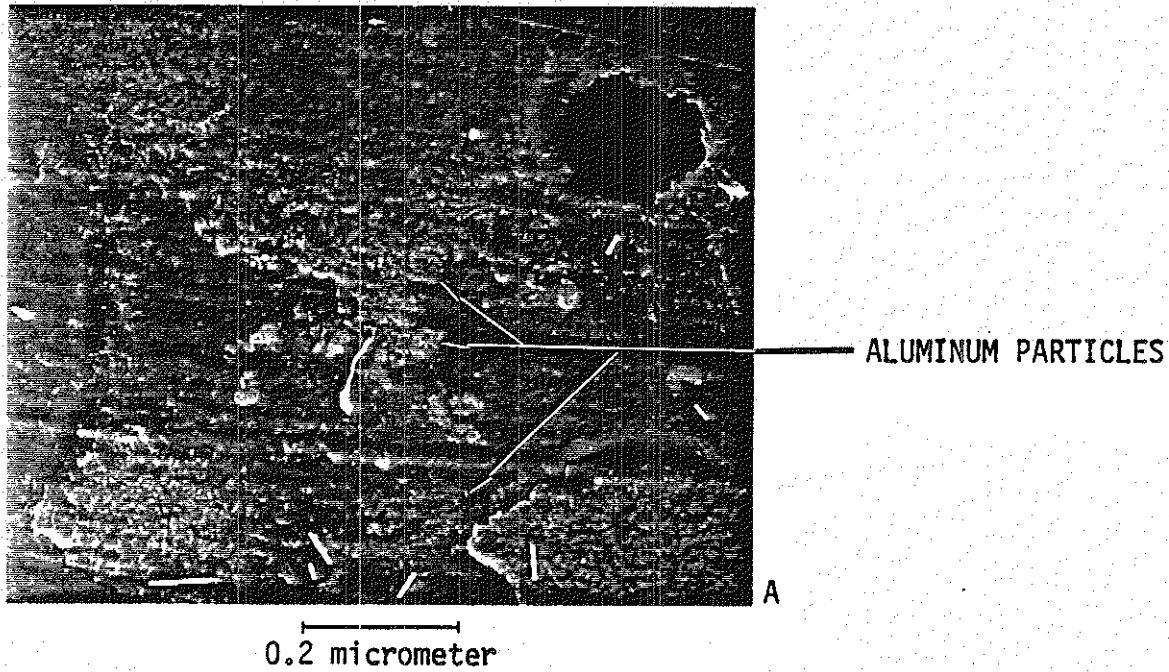
Figure 2.2.3.2-25



0.2 micrometer

10V CAA 10,000 HOURS TEST FAILURE-OXIDE SIDE
STEREO PAIR OF OXIDE WITH NO
POLYMER MATERIAL IN VIEW

Figure 2.2.3.2-26



10V CAA 10,000 HOURS TEST FAILURE-POLYMER SIDE

TOP VIEW OF POLYMER SIDE OF TEST
FAILURE SHOWING (A), ALUMINUM
PARTICLES IN THE POLYMER AND (B),
AREAS OF POLYMER/ALUMINUM PARTICLE
INTERFACIAL PULLOUT.

Figure 2.2.3.2-27

polymer matrix. These are interpreted to be agglomerates of Al particles based on their higher secondary electron yield.

The large, dark region in Figure 2.2.3.2-27a (100X magnification) is a region where polymer has been torn from the adhesive surface. Figure 2.2.3.2-23a represents a surface with a thick adhering polymer layer. Figure 2.2.3.2-27b reveals a localized region of aluminum interfacial separation. The analogous mating fracture on the adherend side is shown as a thin adhering polymer layer in Figure 2.2.3.2-23b.

Further, Figure 2.2.3.2-28 shows a fractured edge of the separation zone in Figure 2.2.3.2-27b. Figure 2.2.3.2-28 also reveals bright nodules ~ 40 nm in diameter that were seen before in PPQ failures on 10V CAA (see Figures 2.2.3.2-7 and 2.2.3.2-8).

Composition

ESCA

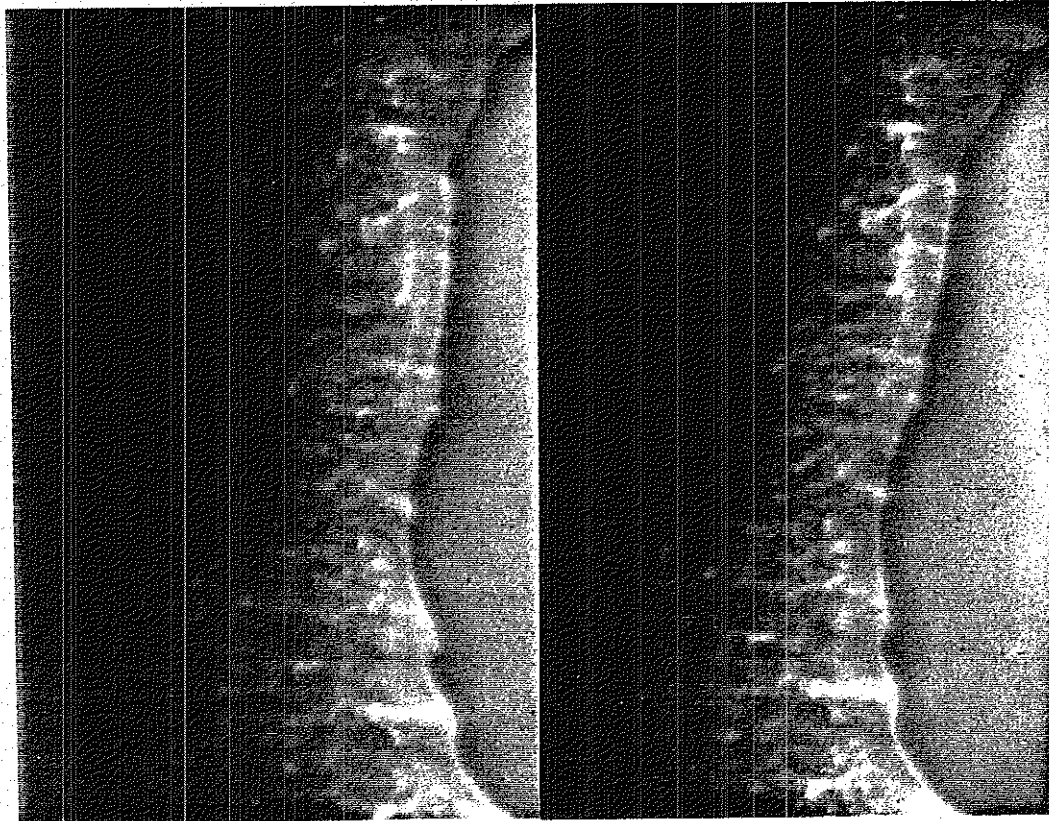
The ESCA surface compositions of the failed 10V CAA/LARC-13 adhesive and adherend are shown in Figures 2.2.3.2-29 and 2.2.3.2-30. The adhesive surface has carbon, nitrogen, oxygen, fluorine, aluminum, silicon, titanium, and chromium. The adherend surface has carbon, nitrogen, oxygen, aluminum, sulfur, titanium, and chromium. The aluminum is due to the filler particles.

The presence of C, N, O on the adherend surface indicates residual polymer. The presence of Ti on the adhesive side indicates transfer of Ti oxide to the adhesive during lap-shear failure.

AES

Figure 2.2.3.2-31 shows an inverted absorbed-current image of an adherend side of the lap-shear failure. The black regions are thick polymer layers, regions C. Regions D represent apparent bare areas. The spectrum from region D showed both Ti oxide and polymer.

Chemical analysis could not be performed on region C alone because the thickness of the polymer layer caused severe charging. To obtain a spectrum including a signal



0.5 micrometer

10V CAA 10,000 HOURS TEST FAILURE-POLYMER SIDE

STEREO PAIR OF TOP VIEW OF A
POLYMER PULLOUT AREA, SHOWING
BRIGHT NODULES ON TOP OF THE
POLYMER

Figure 2.2.3.2-28

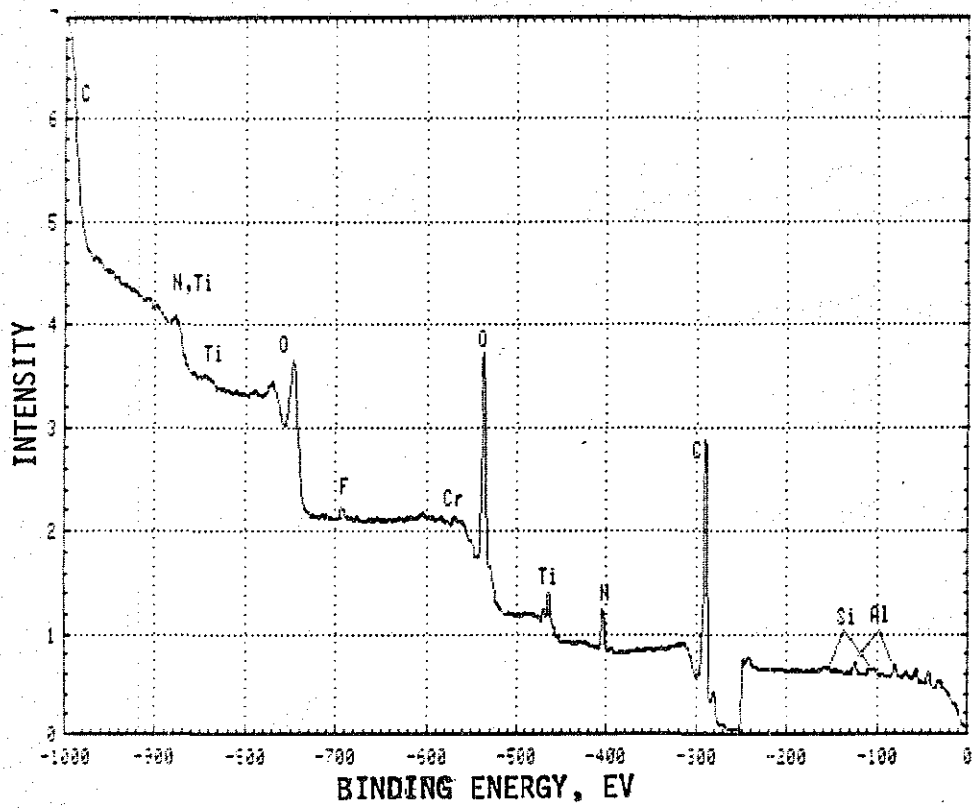


Figure 2.2.3.2-29 ESCA SPECTRUM OF THE FAILED LARC-13/10V CAA LAP SHEAR, ADHESIVE SURFACE

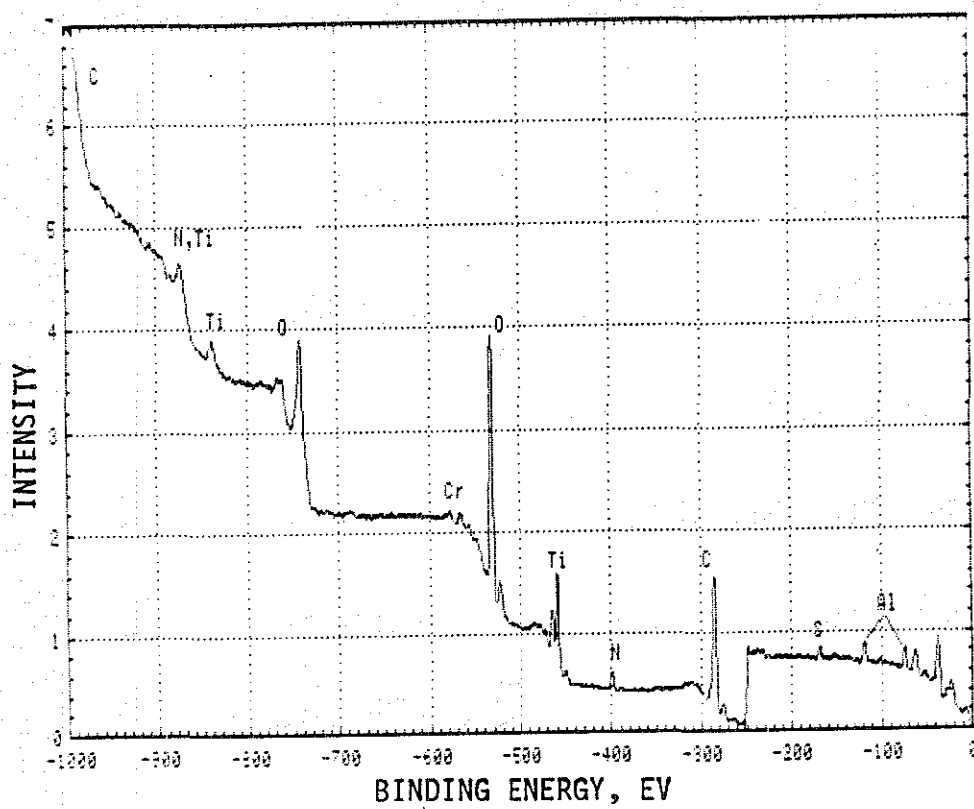
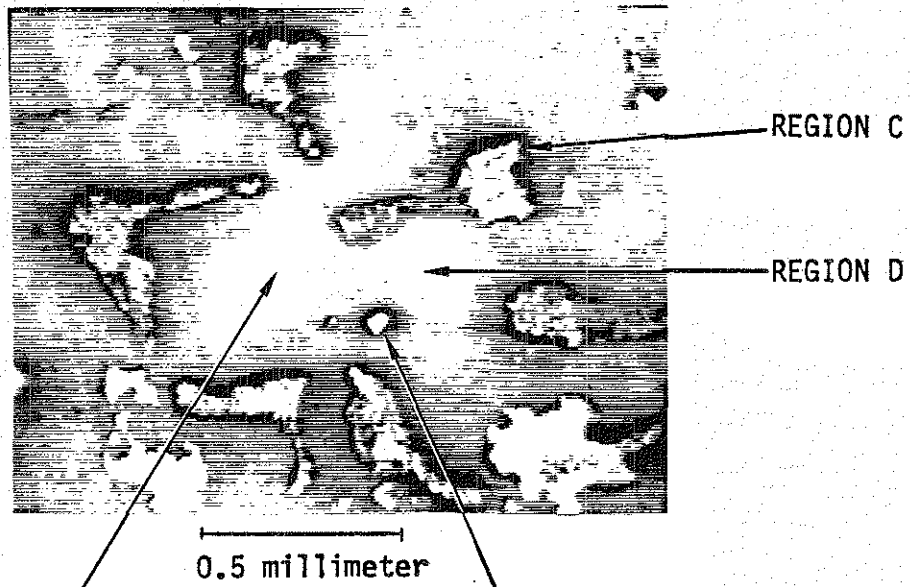
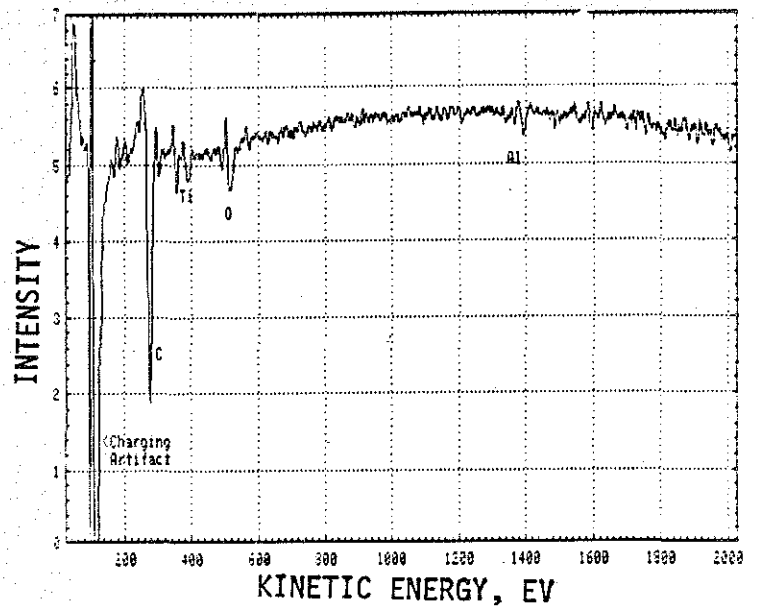
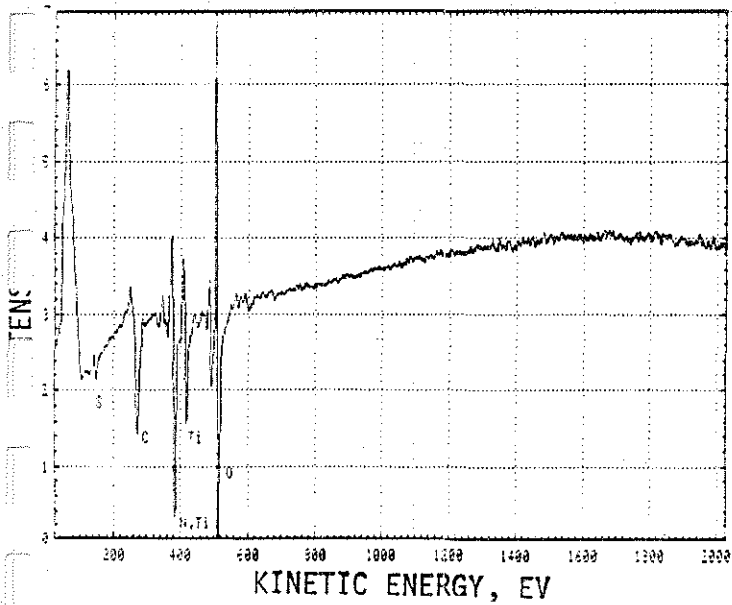


Figure 2.2.3.2-30 ESCA SPECTRUM OF THE FAILED LARC-13/10V CAA LAP SHEAR, ADHEREND SURFACE.



REGION D

REGIONS C & D



AES ANALYSIS OF REGIONS C AND D ON THE LARC-13/10V CAA ADHEREND SURFACE. (50X INVERTED ABSORBED CURRENT IMAGE).

Figure 2.2.3.2-31

from region C, the beam was focused half on region C and half on region D. The resulting spectrum showed a higher signal for C and Al on the composite region than on region D alone.

LARC-13/Pasa-Jell Lap Shear

Morphology

Macroscopic Appearance

The failed lap-shear surface of LARC-13 Pasa-Jell long-term 505K (450°F) is shown in Figure 2.2.3.2-32. The failure mode is identical to that exhibited by LARC-13 10V CAA failure. As in previous LARC-13 failures, scrim node porosity and Al filler particles are present.

Composition

ESCA

The ESCA spectra for the failed surfaces are shown in Figures 2.2.3.2-33 and 2.2.3.2-34. The adhesive surface shows carbon, nitrogen, oxygen, aluminum, silicon, and a trace of titanium. The adherend surface has carbon, nitrogen, oxygen, aluminum, silicon, titanium, and chromium. The trace levels of Ti on the adhesive surface suggest that little Ti transfer occurred during failure, in contrast to the other systems analyzed, with significant Ti signals.

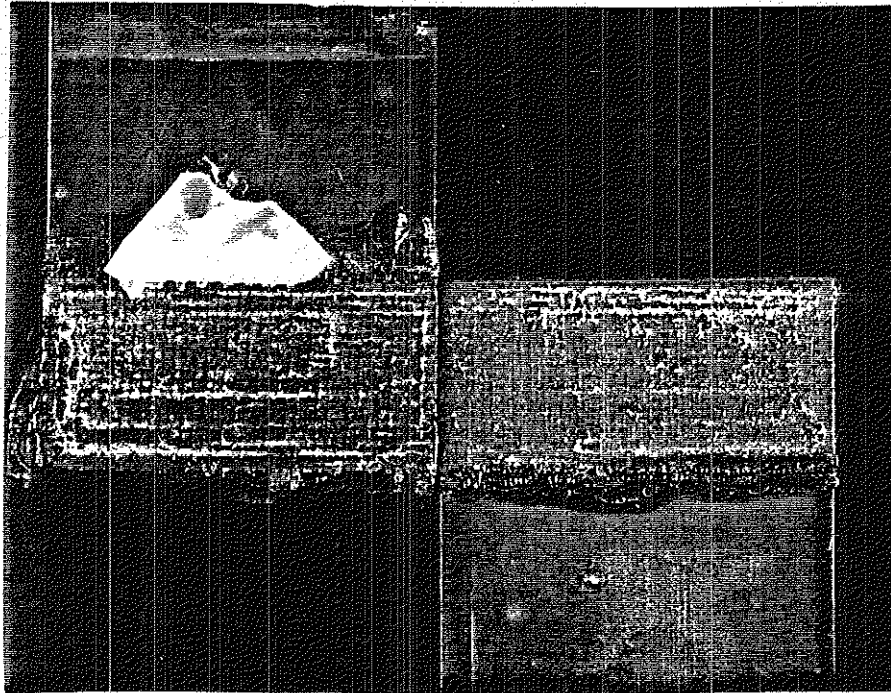
AES

Figure 2.2.3.2-35 shows an inverted absorbed-current image at 50X of the adherend surface of LARC-13 Pasa-Jell lap-shear failure. Region C (white area) represents regions of thick polymer as described for LARC-13 10V CAA. Regions D (grey areas) were bare oxide that AES spectra showed to have C, N, O, and Ti signals. Fluorine, silicon, and sulfur were also detected in the apparent bare area.

Less charging was experienced with these samples, allowing definitive AES analysis of region C showing C, N, O, and Al. They therefore consist of polymer and Al filler

ADHESIVE

ADHEREND



25 millimeter

PHOTOMACROGRAPH OF FAILED LARC-13/PASA JELL LAP SHEAR
THERMALLY AGED AT 505°K (450°F) FOR 10,000 HOURS.

Figure 2.2.3.2-32

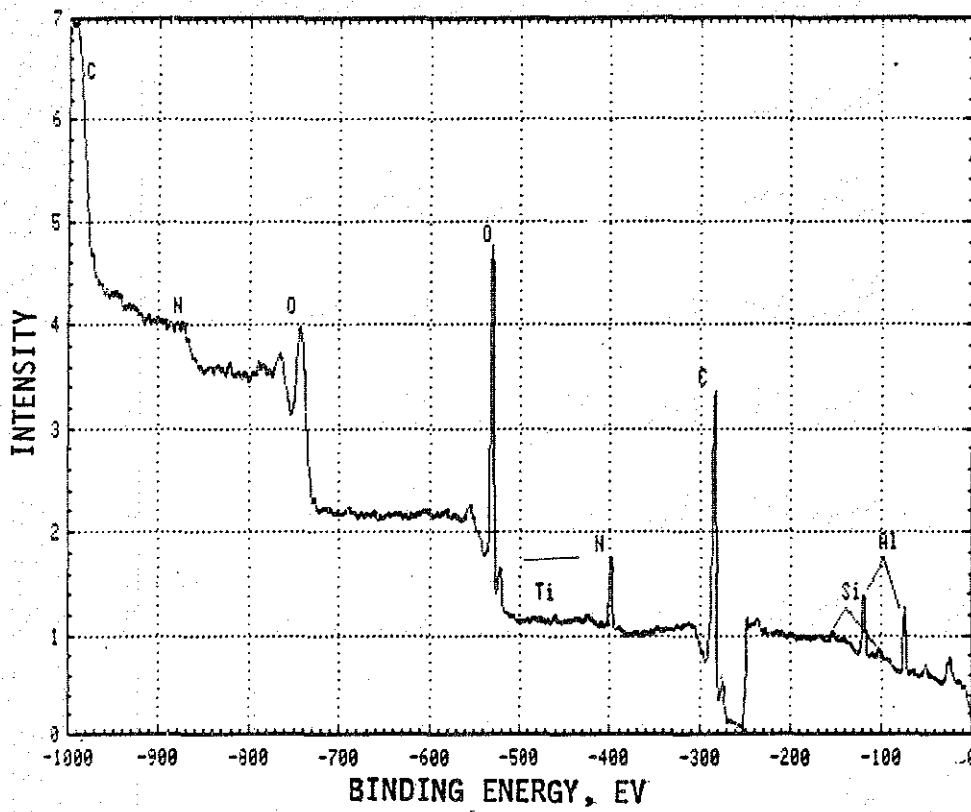


Figure 2.2.3.2-33 ESCA SPECTRUM OF THE FAILED LARC-13/PASA JELL LAP SHEAR, ADHESIVE SURFACE.

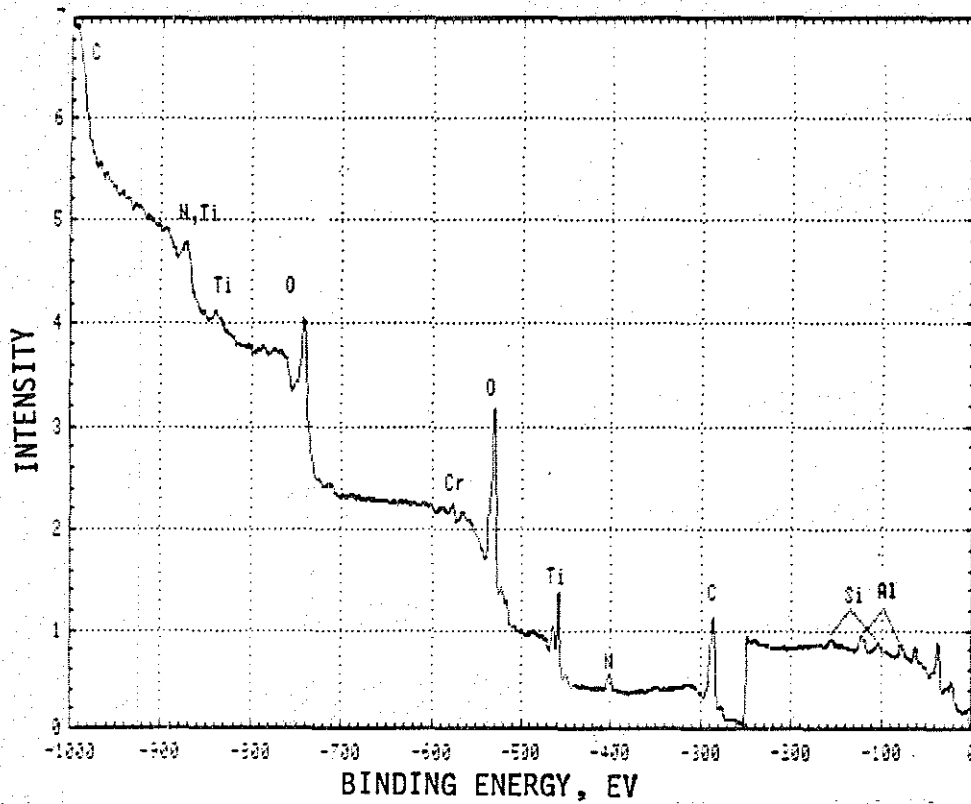
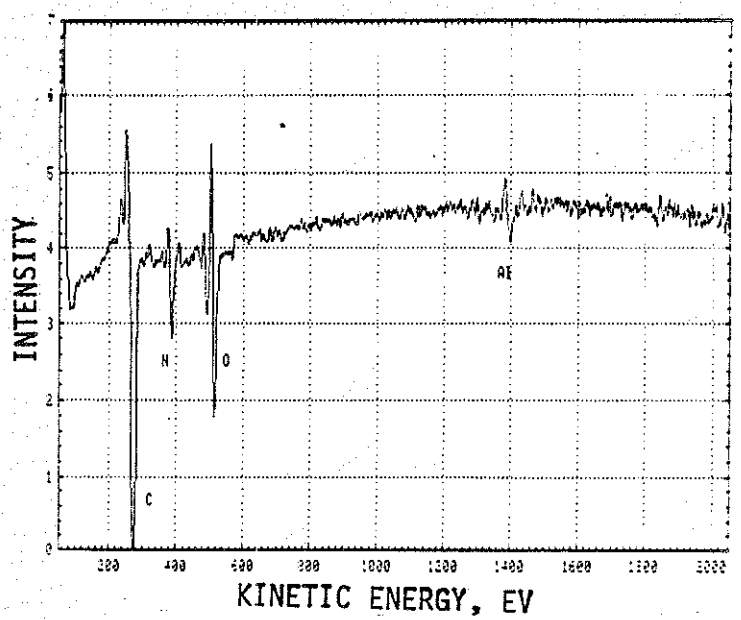
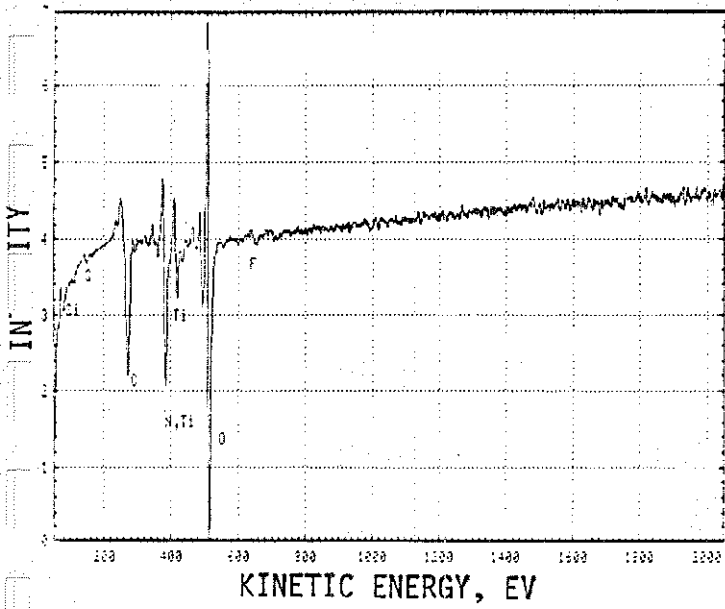
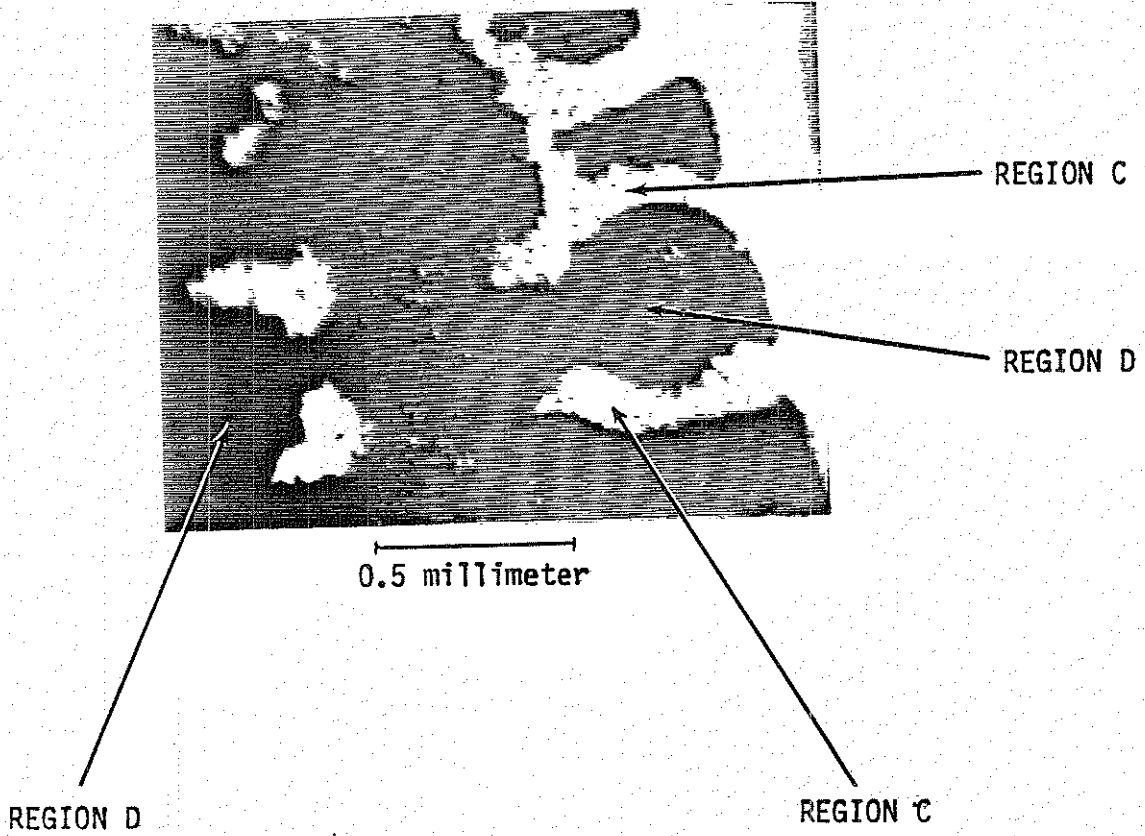


Figure 2.2.3.2-34 ESCA SPECTRUM OF THE FAILED LARC-13/PASA JELL LAP SHEAR, ADHEREND SURFACE.



AES ANALYSIS OF REGIONS C AND D ON THE LARC-13/PASA JELL ADHEREND SURFACE. (50X INVERTED ABSORBED CURRENT IMAGE).

Figure 2.2.3.2-35

particles.

2.2.4 Summary

2.2.4.1 Results

LARC-13 on 10V CAA and PPQ on 5 and 10V CAA

- o LARC-13 and PPQ exhibited extensive bondline porosity both at initial room temperature and after 505K (450° F) thermal aging. Visual examination of failed samples revealed large regions of apparent bare oxide.
- o SEM/STEM plan-view examination of the adherend side revealed mixed regions of exposed oxide with a thin layer of polymer.
- o Both plan and transverse views revealed extensive regions of oxide with no apparent polymer.
- o SEM/STEM examinations of the opposing polymer side revealed good replication of the adherend surface, as well as small 5-nm-diameter nodules.
- o Surface analysis by both ESCA and AES revealed that visually apparent regions of bare oxide on the adherend are composed of titanium and polymer (see Table 2.2.4.1-1 for quantitative results).
- o Analysis of the opposing polymer side similarly revealed both titanium and polymer, with reduced levels of titanium compared to the adherend. In addition, silicon, sulfur, chlorine, and chromium were found in trace amounts.
- o Trace levels of lead were found on both the adherend and opposing adhesive surface on PPQ 5 and 10V CAA samples after thermal aging.

LARC-13 on Pasa-Jell

- o Visual examination of these samples showed large areas of apparent bare adherend.
- o Surface analysis by both ESCA and AES on the adherend surface revealed that apparent bare adherend areas are composed of both polymer and titanium (see Table 2.2.4.1-1 for quantitative analysis).
- o Examination of the opposing polymer surface revealed that it is similarly composed of polymer with trace levels of titanium.
- o Trace levels of sulfur, chlorine, fluorine and silicon were found on both failure

Table 2.2.4.1-1

SUMMARY OF SURFACE COMPOSITIONS AS DETERMINED BY ESCA, IN ATOMIC CONCENTRATION

	C	N	O	F	Al	Si	S	Cl	Ti	Cr	Pb
PPQ/10V CAA Adhesive	72.4	8.6	15.2	ND*	ND	2.3	0.1	0.1	1.1	ND	0.1
PPQ/10V CAA Adherend	63.8	5.6	22.6	ND	0.6	2.5	0.6	ND	4.0	ND	0.3
PPQ/5V CAA Adhesive	73.5	7.9	15.2	ND	0.4	2.0	ND	ND	1.0	ND	0.1
PPQ/5V CAA Adherend	45.3	2.5	37.0	ND	1.6	ND	ND	ND	12.6	ND	1.0
LARC-13/10V CAA Adhesive	68.4	5.5	22.0	0.8	1.0	0.3	ND	ND	1.7	0.2	ND
LARC-13/10V CAA Adherend	49.4	3.3	36.2	ND	2.8	ND	0.5	ND	7.1	0.6	ND
LARC-13/PASA-JELL Adhesive	58.3	8.4	25.7	ND	6.9	0.4	ND	ND	0.2	ND	ND
LARC-13/PASA-JELL Adherend	47.5	4.6	34.5	ND	2.9	1.4	ND	ND	8.2	0.9	ND

* NOTE: ND is defined as element is not detected

surfaces.

2.2.5 Discussion

2.2.5.1 General Behavior

Of the observations on failed long-term 505K (450° F) durability lap-shear specimens, the most important is the shift from a cohesive failure with no visually exposed oxide to an apparently adhesive failure with exposed oxide visible. The lack of base plate, oxide, or cohesive polymer fracture clearly indicates that the overall basic oxide and polymer are more stable than the bond between them, whether the bond is primarily chemical or mechanical. For the polymer, this observation is reinforced by the reproducibility of stable glass transition behaviors, even after 10,000 hours of aging at 505K (450° F).

Also significant in this overall trend from cohesive to adhesive failure is the observation of scrim node porosity. Detailed examination of room-temperature-tested lap-shear specimens revealed a generally cohesive fracture. Scrim node porosity was evident at the primer/adhesive bondline. Because the path of cohesive failure on these samples avoided the bondline, the existence of bondline porosity is not considered to be a significant aspect of fracture. As shown in Figure 2.2.3.2-2, the typical adhesive fracture after long-term aging exhibits 25-50% total area porosity. Such an observation suggests that the true stress seen by the interfacial bond with this failure mode is actually 25-50% higher than the calculated engineering stress. This result may be significant in the comparison of thermal degradation rates between polymer systems exhibiting adhesional fracture behavior.

PPQ on 5 and 10V CAA and LARC-13 on 10V CAA

Long-term durability failures on PPQ on 5 and 10V CAA and LARC-13 on 10V CAA can be considered jointly, both on the basis of the generic similarity of 5 and 10V CAA, and on their apparently identical failure morphologies and chemistries. The morphology of failed specimens over a range of magnifications continues to define the locus of failure within the top 4nm of the oxide tips. The lack of severe deformation of either oxide or polymer indicates a relatively low-energy adhesional failure. The suggestion of an interfacial separation is supported by the

detailed replication of oxide surface details down to 5.0nm.

Plan and transverse views of the failed adherend surface revealed a general lack of polymer within the CAA oxide structure. This observation suggests poor polymer penetration into the oxide. However, detailed examinations of primed control samples revealed that good polymer penetration does in fact occur in these systems. The subsequent interpretation is that polymer penetration probably did occur, and that the small 5.0-nm nodules noted on the opposing polymer surface represent relaxed polymer pulled out of the CAA oxide porous structure. The interpretation of the nodules as polymer pulled out of the porous structure is primarily based on Boeing experience indicating that large amounts of polymer strain relaxation are possible.

ESCA and AES surface chemical analysis techniques clearly indicated titanium and polymer on both the adherend and adhesive surfaces.

The SEM/STEM results showed intact oxide morphology on the adherend side and no apparent oxide on the adhesive side.

Detailed TEM/STEM/EDX analysis of thin sections of the adhesive fracture surface indicated that the titanium detected by ESCA must be present as several monolayers, rather than as discrete thicker regions. Transfer of several monolayers of titanium oxide to the adhesive side during fracture is not inconsistent with an interfacial failure mode. The detection of Si, Cl, S and Cr on the adherend failed surfaces also supports an interfacial failure interpretation since these elements were detected on baseline oxide studies, (Third Semi-Annual Progress Report, May 1980). The existence of Pb on PPQ/CAA long-term durability failures was briefly discussed in Section 2.2.3. Since Pb was not found on baseline CAA oxide studies, the PPQ must be the source of the Pb detected. However, the similarity in failure morphology and surface chemistry on both LARC-13 and PPQ failures strongly suggests that lead, detected in amounts less than 1 atom percent, is not principally related to long-term adhesional failures in the systems studied.

LARC-13 On Pasa-Jell

In general, the failure analysis results on Pasa-Jell/LARC-13 long-term 505K (450° F) durability samples appeared very similar to those characterized on LARC-13 and PPQ

CAA long-term durability failures. Although no SEM/STEM analyses were performed, the surface chemical data by AES and ESCA is clearly very similar to those results for CAA related failures. Both the adherend and adhesive surfaces exhibit combined polymer and titanium signals, with the level of titanium detected on the polymer surface significantly lower than that on the adherend. These results, as with CAA, suggest fracture of an ahesional nature with some minor titanium monolayer transfer.

2.2.5.2 General Discussion of Results

The proper interpretation of failed sample morphologies and chemistries requires that features observed be interpreted with respect to requirements for bond joint strength and durability. Adhesive bonding is generally well recognized to occur as a result of mechanical interlocking combined with interfacial chemical bonding. The aspect of bonding determining bond joint strength generally depends on a number of variables, including polymer/oxide chemistry, polymer flow, and adherend surface structure. The general approach in bond joint optimization involves improvement of either mechanical interlocking or chemical bondability. Pasa-Jell and 10V CAA surface preparations represent generic extremes of these conditions on titanium. Pasa-Jell typifies a surface-cleaning type of preparation in which chemical bondability provides the dominant source of bond strength. On the other hand, 10V CAA represents the generic extreme of a mechanical interlocking type of bonding in which a large surface area, columnar oxide structure is generated.

A review of Table 2.2.5.2-1 indicates that for PPQ, LARC-13, and NRO56X, significant increases in bond joint strength are obtainable at room temperature by increased mechanical interlocking. It should not be forgotten that differences in surface chemical compositions will also influence bond strength.

In 5V CAA, or any of the reduced structure oxides, interim optimization levels are represented, where the reduction of mechanical bond surface area places an increasing emphasis on chemical bondability. Even an apparently improved system such as 10V CAA may still represent an interim compromised bonding state.

Thermal aging represents an additional perturbation of bond joint integrity. Thermally activated processes occur by which either chemical or mechanical bonding levels can be degraded. However, the extent to which the actual bond joint integrity is

Table 2.2.5.2-1

Lap-shear Strength vs. Surface Preparation
Tests Performed at Room Temperature in Task I

Adhesive	10VCAA	5VCAA	Pasa-Jell
PPQ	5.3	1.8	---
LARC-13	2.9	---	0.8
NR056X	4.2	---	1.10

Values in Ksi

diminished will be largely a function of which bonding aspect is degraded.

The failure analysis performed thus far on PPQ on 5 and 10V CAA and LARC-13 on 10V CAA and Pasa-Jell clearly suggest failure induced by a lack of chemical cohesion. The surface chemistries exhibited by both Pasa-Jell and 10V CAA indicate that the failure plane is at the immediate oxide/polymer bond interface. Additionally, the SEM/STEM analyses performed demonstrate that no gross morphological oxide structure changes have occurred and that failure is, for the most part, interfacial to the extent that polymer pull-out has even occurred. This conclusion is reinforced by the strong similarity in failure mode exhibited by LARC-13 on 10V CAA and Pasa-Jell, each relative surface optimization extremes.

2.2.5.3 Conclusions

The failure analysis performed indicates that long-term 505K (450° F) durability failures are chiefly related to chemical bond durability. The investigations described in this report have not enabled the causes of the bond degradation to be identified.

The fracture characteristics demonstrated interfacial failures on thermally aged samples on which surface chemistry and surface contamination represent major factors.

The results described suggest that the mechanical properties of the bond may be improved by modifications of the surface chemistry and the elimination of surface contamination. The techniques described in this report, together with developments and improvements, can be applied to such an optimization study.

2.3 PHASE II—TASK II ENVIRONMENTAL EXPOSURE DATA

2.3.1 General Discussion

This portion of the program is evaluating environmental effects of high temperature/humidity, fuels and fluids, thermal (stressed and unstressed) and thermal cycling upon PPQ and LARC-TPI adhesive systems.

TABLE 2.3-1. Unstressed Thermal Aging, LARC-TPI

Data Summary

Test Coupon	Test Temperature, K (°F)	Exposure Time				
		Initial	100 HR	500 HR	1000 HR	2000 HR
Lap Shear, MPa (Psi)	219 (-65)	32.6 (4760)	--	--	31.5 (4570)	TBD
	Ambient	29.7 (4310)	--	--	25.2 (3660)	TBD
	422 (300)	23.6 (3420)	--	--	23.3 (3380)	TBD
	505 (450)	14.8 (2150)	--	--	19.7 (2862)	TBD
	533 (500)	7.0 (1020)	--	--	-- --	--
T-Peel, N.M (lb/in)	219 (-65)	0.41 (3.6)	--	--	0.45 (4.0)	TBD
	Ambient	0.51 (4.5)	--	--	0.38 (3.4)	TBD
	422 (300)	0.41 (3.6)	--	--	0.31 (2.8)	TBD
	505 (450)	0.81 (7.2)	--	--	0.6 (4.6)	TBD
	533 (500)	1.02 (9.0)	--	--	-- --	--
Crack Extension, mm (inches) growth	219 (-65)	0.25 (0.01)	1.52 (0.06)	1.78 (0.07)	1.78 (0.07)	TBD
	Ambient	0.00 (0.00)	1.02 (0.04)	1.02 (0.04)	1.78 (0.07)	TBD
	422 (300)	0.76 (0.03)	1.78 (0.07)	2.03 (0.08)	2.54 (0.10)	TBD
	505 (450)	1.52 (0.06)	2.79 (0.11)	3.05 (0.12)	3.56 (0.14)	TBD
	533 (500)	5.08 (0.20)	9.65 (0.38)	-- --	-- --	TBD

Test coupons for LARC-TPI have reached 1000 hours aging at 505K (450°F). Table 2.3-1 lists the LARC-TPI unstressed thermal aging test results to date. Data for PPQ was reported in the May 1981 Semi-Annual progress report.

2.3.2 Stressed Thermal Aging

These tests are designed to facilitate the prediction of 50,000-hour service at 505K (450°F) by exposing lap-shear specimens under load for varying periods of time and then testing for residual strength. From these data, a plot of residual strength versus time will be made for each stress level and temperature tested. From the trends, a prediction of long-term performance will be attempted.

Lap-shear specimens are being loaded to 25 and 30% of ultimate stress at 219 (-65°F), ambient and removed and tested for residual strength at the exposed temperature. The time intervals indicated may vary depending upon the results of the stress-rupture data from Task I and as data are accumulated from these tests. Three lap-shear specimens are being tested for each data point. Data for PPQ is presented in Table 2.2-2. There appears to be no difference between the 25 percent and 30 percent stressed coupons. The 450°F exposed coupons still exceed 2300 psi lap shear at 3000 hours. LARC-TPI specimens are currently being exposed and are not yet tested.

2.3.3 Humidity Exposure

PPQ lap-shear, T-peel, and crack-extension specimens have been exposed for 2,000 hours in a humidity cabinet under conditions of 322K (120°F) and 95% RH. Specimens were removed and immediately tested at 219K (-65°F), ambient, and 505K (+450°F) for exposure conditions of 1,000 and 2,000 hours (five specimens per data point). Lap-shear strength, T-peel strength, and crack-extension length were recorded, as well as the mode of failure. This data was reported in the May 1981 Semi-Annual progress report. Table 2.3-3 lists the data for LARC-TPI generated thus far.

2.3.4 Aircraft Fluid Exposure

The resistance of the adhesives to common aircraft fluids is being assessed. Lap-shear and crack-extension were submerged in selected fluids as follows:

1. JP-4 jet fuel, ambient

TABLE 2.2-2. Stressed Thermal Aging--PPQ
Data Summary - Lap Shear

Test Temperature K (°F)	Percent Load	Exposure Time							
		0 hour		100 hours		1000 hours		3,000 hours	
		<u>MPa</u>	<u>psi</u>	<u>MPa</u>	<u>psi</u>	<u>MPa</u>	<u>psi</u>	<u>MPa</u>	<u>Psi</u>
219 (-65)	25 8.28 MPa (1200 psi)	29.8	(4320)	34.9	(5060)	37.7	(5460)	30.3	(4390)
	30 10.3 MPa (1500 psi)	30.6	(4440)	34.0	(4930)	36.5	(5290)	32.1	(4650)
Ambient	25 8.28 MPa (1200 psi)	31.2	(4520)	33.7	(4890)	31.3	(4540)	28.7	(4160)
	30 10.3 MPa (1500 psi)	33.5	(4860)	34.6	(5010)	34.6	(5010)	28.8	(4180)
505 (450)	25 5.1 MPa (740 psi)	20.4	(2960)	21.3	(3090)	19.8	(2870)	16.2	(2350)
	50 10.2 MPa (1480 psi)	19.6	(2840)	22	(3190)	21.3	(3090)	16.7	(2420)

TABLE 2.3-3. Humidity Exposure - LARC-TPI

322K (120°F)/95% RH

Data Summary

Test Coupon	Test Temperature, K (°F)	Exposure Time	
		1000 Hours	2000 Hours
Lap Shear, MPa (Psi)	219 (-65)	26.8 (3900)	TBD
	Ambient	16.4 (2380)	TBD
	505 (450)	14.5 (2100)	TBD
T-Peel, N.M (lb/in)	219 (-65)	0.34 (3.0)	TBD
	Ambient	0.29 (2.6)	TBD
	505 (450)	0.47 (4.2)	TBD

2. MIL-H-5606 hydraulic fluid, ambient and 344K (160°F)
3. Skydrol hydraulic fluid, ambient and 344K (160°F)
4. MIL-H-7808 lubricant, ambient
5. Deicing fluid, ambient

PPQ specimens were tested after 30 and 60 days exposure at ambient temperature for all fluids. In addition, tests were conducted after 30 and 60 days 344K (160°F) exposure to MIL-H-5056 and Skydrol exposure and test at ambient for all fluids for up to 5,000 hours will be conducted.

PPQ data to 5000 hours is shown in Table 2.3-4 LARC-TPI data to 60 days is shown in Table 2.3-5.

2.3.5 Extended Exposure

To permit NASA to obtain 50,000-hour aging data on lap-shear specimens, Boeing will fabricate 100 extra lap-shear specimens and 12 crack-propagation specimens at the same time that the stressed and unstressed thermal aging specimens are fabricated. Specimens will be inserted into the aging chamber at 505K (450°F) in an unstressed condition and in a stressed (50% of ultimate) condition at the same time that the initial aging specimens are started. If NASA elects to extend the contract and continue the aging program after the 36-month contract period, the specimens will be removed and tested at appropriate time intervals (e.g., 10,000; 20,000; 30,000; 40,000; and 50,000 hours). If the contract is not extended, all specimens will be delivered to the NASA project monitor.

2.3.6 Thermal Cycling

Lap-shear, T-peel, and crack-extension specimens will be thermally cycled from 219K (-65°F) to 505K(+450°F) at the rate of 30 minutes per cycle. Specimens will be tested after 1,000 and 2,000 thermal cycles. Five lap-shear and five T-peel specimens will be tested for residual strength at ambient and 505K (450°F); the crack-extension specimens will be examined and measured for crack propagation at each time interval.

TABLE 2.3-4. Aircraft Fluid Exposure, PPQ

Test Coupon	Duration	JP-4 Ambient	MIL-H-5606		Skydrol		MIL-H-7808 Ambient	Deicing Fluid Ambient
			Ambient	344K (160°F)	Ambient	344K (160°F)		
Lap Shear, MPa (Psi)	30 days	33.0 (4780)	32.1 (4660)	35.3 (5120)	34.7 (5030)	26.3 (3810)	27.7 (4020)	33.3 (483)
	60 days	32.8 (4750)	30.8 (4470)	35.0 (5080)	30.6 (4430)	26.3 (3810)	33.0 (4780)	34.7 (503)
	5000 Hr	(4190)	(4330)	--	(4030)	--	(4270)	(466)
Crack Extension, mm (inches) growth	30 days	3.3 (0.13)	3.3 (0.13)	5.6 (0.22)	18.5 (0.73)	31.8 (1.25)	13.2 (0.52)	3.8 (0.1)
	60 days	3.3 (0.13)	9.1 (0.36)	6.8 (0.27)	19.6 (0.77)	33.8 (1.29)	13.2 (0.52)	3.8 (0.1)
	5000 Hr	(0.15)	(0.37)	(0.32)	(0.78)	(1.61)	(0.54)	(0.1)

TABLE 2.3-5 Aircraft Fluid Exposure, LARC-TPI

Test Coupon	Duration	JP-4 Ambient	MIL-H-5606		Skydrol		MIL-H-7808 Ambient	Deicing Fluid Ambient
			Ambient	344K (160°F)	Ambient	344K (160°F)		
Lap Shear, MPa (Psi)	30 days	27.7 (4020)	26.4 (3830)	31.6 (4590)	29.1 (4220)	21.0 (3040)	29.0 (4210)	27.2 (3950)
	60 days	27.9 (4050)	29.0 (4210)	27.9 (4050)	27.4 (3970)	20.3 (2950)	26.1 (3790)	26.7 (3870)
Crack Extension, mm (inches) growth	30 days	1.78 (0.07)	2.79 (0.11)	3.05 (0.12)	3.30 (0.13)	10.7 (0.42)	2.29 (0.09)	4.06 (0.16)
	60 days	3.05 (0.12)	3.30 (0.13)	3.56 (0.14)	4.3 (0.17)	14.0 (0.55)	3.05 (0.12)	5.84 (0.23)

3.0 PROGRAM STATUS

3.1 PHASE I—ADHESIVE SCREENING

- o Ten candidate adhesive systems were selected as specified in the contract statement of work section 3.1.A.
- o Eight different Ti-6Al-4V surface treatments have been investigated for each of the 10 adhesive resins per statement of work section 3.1.B.
- o Primers (two for each adhesive resin) have been investigated for appropriate cures and thickness per statement of work section 3.1.C.
- o Initial evaluation of bonded joints using various combinations of the above adhesive resins and surface treatments has been completed per statement of work section 3.1.D.
- o Selection of four adhesive systems (primer, adhesive resin, and surface treatments) per statement of work section 3.1.E was attempted. However, based upon the data generated during initial evaluation, the three systems selected represent the major types of adhesive systems (i.e., PPQ, condensation polyimide, and additional polyimides presently available. Evaluation of these candidates should yield data that are representative of their types of polymers). This decision was reached with the concurrence and approval of the NASA Technical Representative of the Contracting Officer.
- o One lap-shear adherend surface-treated and primed by each process was shipped to Dr. Jim Wightman of Virginia Polytechnic Institute per statement of work section 3.B.
- o Cure cycle optimization studies for each adhesive system per statement of work section 3.1.E(1) have been completed.
- o Properties versus temperature have been completed on each adhesive system per statement of work section 3.1.E(2), except for T-peel coupons, which were removed from the test matrix. T-peel was replaced with hand peel for each system at room temperature with concurrence of the NASA Technical Monitor.
- o Thermal aging characteristics per statement of work section 3.1.E(3) have been initiated. Aging has been completed through 10,000 hours.
- o Humidity aging characteristics per statement of work section 3.1.E(4) have been initiated. Aging has been completed through 5,000 hours.
- o Large-area bonding per statement of work section 3.1.F has been completed.

- o Surface characterization and failure analysis per statement of work section 3.1.G have been completed for PPQ.
- o Fractured lap-shear specimens per Part IX, Delivery, Item Description No. 1 have been shipped to Virginia Polytechnic Institute and State University.
- o Fractured lap-shear specimens per statement of work section 3.1.B have been delivered for surface characterization and failure analysis per statement of work section 3.1.G.
- o NR056X and PPQ were selected for continued evaluation in Phase II.
- o LARC-2 (LARC-TPI) was added to Phase II evaluation.

3.2 PHASE II—ADHESIVE OPTIMIZATION AND CHARACTERIZATION

- o Phase II Task I, per statement of work section 3.2, has been initiated.
- o Adhesive resin batches of PPQ and NR056X have been received and chemical analysis completed per statement of work section 3.2.A.
- o Titanium sheet required for test coupons in Phase II has been received.
- o Optimization of formulation, process, and surface treatment is in progress for PPQ, LARC-2 (LARC-TPI), and NR056X.
- o Rough draft material and process specifications have been prepared for PPQ and LARC-2 (LARC-TPI).
- o Cure cycle thermal aging data, 505K (450°F) to 3,000 hours, have been completed.
- o NR056X is being dropped from the program.
- o Phase II Task II per statement of work section 3.2.B has been initiated for PPQ.
- o Stressed thermal aging to 3,000 hours has been completed for PPQ.
- o Unstressed thermal aging to 1,000 hours has been completed for PPQ.
- o Humidity aging to 2,000 hours has been completed for PPQ.
- o Aircraft fluids exposure to 5,000 hours has been completed for PPQ.
- o Extended exposure has been initiated for PPQ.
- o Unstressed thermal aging to 1,000 hours has been completed for LARC-TPI.
- o Humidity aging to 1,000 hours has been completed for LARC-TPI.
- o Aircraft fluids exposure to 60 days has been completed for LARC-TPI.
- o Extended exposure has been initiated for LARC-TPI.

4.0 WORK PLANNED FOR NEXT 6 MONTHS

- o Continuation of Phase II aging for PPQ and LARC-TPI
- o Continue surface failure analysis as necessary.

REFERENCES

1. E. A. Ledbury, A. G. Miller, P. D. Peters, E. E. Peterson and B. W. Smith, "Microstructural Characteristics of Adhesively Bonded Joints". 12th National SAMPE Conference. October 1980.

End of Document